Geosciences and Geological and Petroleum Engineering Faculty Research & Creative Works

Geosciences and Geological and Petroleum Engineering

27 Dec 1972

Investigation of present thermal regime of Missouri River in Missouri

James C. Maxwell
Missouri University of Science and Technology

Recommended Citation

INVESTIGATION OF PRESENT THERMAL REGIME OF MISSOURI RIVER IN MISSOURI

PRINCIPAL INVESTIGATOR: James C. Mawell
Department of Geology

UNIVERSITY OF MISSOURI - ROLLA

PROJECT No.   B-045-Mo.

AGREEMENT NO.   14-31-0001-3299

DATE: 7-1-70 thru 1-31-72

COMPLETION REPORT - December 27, 1972

ABSTRACT

The applicability of power spectral density techniques, Fourier series analysis, and linear regression to the mathematical modeling of river water temperature is demonstrated. Consideration is also given to the problem of estimating thermal inputs to rivers from man-made sources such as electrical power plants. First, power spectral density techniques are used in the time-series analysis of water temperature records which were taken from the Missouri River. Two spectral ranges are then studied from the standpoint of their applicability to (1) mathematical model building and (2) detection and identification of cyclic thermal inputs. Next, a Fourier regression fit to the time-series data is used to show that normal random variates having zero mean are obtained when the regression curve is extracted from the data. A 60-day prediction of daily-average water temperature is then made using a model which is based upon a polynomial regression fit to the fluctuating amplitudes of significant Fourier components. A final predictive model, which is based on the above analysis methods, is proposed.

TABLE OF CONTENTS

Page

LIST OF ILLUSTRATIONS

LIST OF TABLES

I. INTRODUCTION

A need has been established [1] for the use of both deterministic and probabilistic techniques in the development of prediction models for river water temperatures. A corresponding need exists for similar techniques in the estimation of man-made thermal inputs to large rivers. These needs are based on the concern which has recently developed [2,3,4,5,6] as a result of projected large increases in nuclear and fossil-fuel production of electrical power in the United States. A commonly quoted statement is that "the demand for electric energy in the United States is doubling every decade." Obviously there are physical limitations on the number of electrical power plants which can be built. However, this does not diminish the concern for the damaging effects to the ecological patterns which these power plants are likely to cause in our nation's large rivers.

The reason for this concern is that very large amounts of water are usually required for cooling purposes in both nuclear and fossil-fuel electrical power plants. Also, both operate at relatively low thermal efficiency. Typical efficiency ratings are 20 to 35 percent for nuclear reactors and 40 to 50 percent for fossil-fuel power plants. Thus, the power generation process results in the discharge of large amounts of heated water back into the nation's rivers. As an example, the rise in water temperature which typically results from the operation of a 500-megawatt nuclear plant is 8 to 10° at the plant site. Ecologists and biologists are

concerned that a continued increase in these thermal inputs from an ever increasing number of power plants might destroy beneficial aquatic life while at the same time attracting both undesirable flora and predatory aquatic fauna.

One of the criteria which is specified by water quality control boards for the thermal output of electrical power plants is that the water temperature shall not exceed a certain level above the natural water temperature. The question is immediately raised in regard to what constitutes the natural water temperature. To a large extent this question is ignored for lack of an answer. Obviously there is already some degree of thermal pollution present in our larger rivers as a result of both waste discharges and thermal discharges from presently existing electrical power plants.

In order to assess the temperature effects of future thermal inputs it is necessary to determine, insofar as possible, the present and the past thermal properties of the nation's rivers. The objective of this project was developed as a result of a study of the requirements for establishing a basis on which these temperature effects can be ascertained. The problem is to:

   (1) establish, by means of power spectral density techniques, whether any periodicities (other than the yearly seasonal cycle) of significant level exist,

   (2) determine a means whereby future thermal input levels can be estimated, and

(3) build a mathematical model which will predict

future water temperatures.

A major contribution of this project is presented in
Chapter III where power spectral density techniques are
used to obtain the spectral characteristics of fluctuations
in river water temperature. The fluctuations studied include
those which occur at frequencies near the one cycle/year
seasonal fluctuation as well as those at higher frequencies
of up to 400 cycles/year.

In order to obtain the desired results at frequencies
near the one cycle/year fluctuation, it was necessary to
consider some means of extracting this large cyclic component.
To do this, a least-squares Fourier series regression fit to
the time-series data was used. Both the average component
and the one cycle/year component were then subtracted from
the raw data to yield a residual data set. This residual
data set was then spectrally analyzed in order to obtain
information about the existence of cyclic fluctuations other
than the one cycle/year component.

In Chapter IV consideration is given to the possibility
of utilizing communication theory methods in the detection of
thermal inputs to large rivers. Study and analysis of this
problem indicated that a mathematical model which would make
possible the prediction of river water temperature would be
more appropriate.

This conclusion was based on the fact that an obvious
criterion which had already been taken into account by pollu-
tion control boards was the setting of a maximum allowable

increase in water temperature. Thus, the prediction of above-normal water temperature, particularly over the summer months, would be an invaluable aid to such agencies as well as to electrical power companies. The final form for the mathematical model consists of four component parts. These are:

 (1) the slowly varying yearly average water temperature,

 (2) Fourier components which make up the very large yearly seasonal fluctuation of water temperature,

 (3) short-term cyclic fluctuations, called wavelets, and

 (4) a normal random process with zero mean.

One of the reasons for selecting this problem was its timeliness. It is evident by the concern presently being given to our environment that the nation's technological achievements must now be tempered through the use of techniques such as those which are presented in this report.

indirectly supported these studies through a Gulf Oil Fellowship to the junior investigator.

II. REVIEW OF LITERATURE

The advent of the present ecological crisis in the United States has resulted in a myriad of scientific investigations into the potential dangers to all phases of marine plant and animal life as a result of thermal pollution. Many papers have been written which are based on specific investigations into the potential dangers to marine plant and animal life through elevated water temperature. These papers establish the need for the implementation of controls on man-made thermal inputs to our rivers and lakes but, by their nature, they do not determine how the controls are to be effected.

The effective implementation of such controls on large rivers will have to be based upon a thorough knowledge of the thermal properties of these rivers. Previous investigations of these thermal properties can be placed in four rather broad categories. These are:

(1) Direct observation and compilation of existing temperatures.

(2) Physical Model-building of thermal inputs.

(3) Analytical Model-building.

(4) Model-building based on the water temperature fluctuation when considered strictly as a time-series.

The first category includes various types of water temperature data, but primarily it consists of average water

temperature calculations which are tabulated on either a daily average or a monthly average basis. A typical example is the table of daily average water temperatures for the Missouri River at Boonville, Missouri, which was supplied by the U.S.G.S. for this study.

In the second category, much of the model-building has been based upon the use of laboratory models. For example, McAllister, Lawrence, and Bradfield [7] constructed a model of an Ohio River power plant site consisting of a power plant with cooling tower. Heated water was discharged from the cooling tower into an inlet channel which was formed by an island. The water was thus mixed to some extent before final mixing occurred in the main channel of the river. A very thorough analysis of the resulting temperature isotherms was presented in the paper. These results demonstrated that an upper layer of lighter warm water is formed at the source of thermal input. From that point gradual mixing continues at the interface of the warm upper layer and the underlying cold water until a fully mixed temperature is reached.

Some excellent model-building results were also obtained by Nobuyuki, Wiegel, and Tornberg [8]. They constructed a cold-water plume into which warmer water was injected by means of a warm-water jet. The results demonstrated that the concept of an analogy between the thermal input and a communication-system antenna is valid since the temperature isotherms had the appearance of typical antenna power patterns. The vertical pattern results substantiated the

results presented by McAllister which showed the formation
of the surface layer of warm water with slow mixing at the
cold-water interface. These results were obtained under
ideal conditions and hence do not account for mixing effects
caused by stream turbulence.

As an example of the results obtained from the physical
modeling of thermal inputs, Jaske [9] reproduces the equation:

$$L = \kappa \cdot \frac{5280}{\overline{W}} \cdot \overline{V}^{1/2} \cdot (G \cdot W_e)$$

where

        L = affected river length (miles),

       $\overline{W}$ = average river width (feet),

       $\overline{V}$ average stream velocity (ft/sec),

    $G \cdot W_e$ = power plant rating (watts), and

      κ = proportionality constant.

Typical results which were obtained using this equation
showed that L is equal to 10 miles for slow moving streams
where the plant input is taken as 10^9 watts.

A considerable amount of work in the area of analytical
model building (category 3) of thermal inputs has been based
on what is called the energy budget method. Essentially
this method consists of taking an account (or budget) of all
possible thermal sources, both input and output, and forming
a resultant sum of the total quantity of heat. Applications
of this method were made by Brown [10] for the prediction of
water temperature in small streams. Also, Morse [11] used
this method to build a mathematical model for stream tempera-
ture predictions for larger rivers.

Further analytical work has been done very recently by Chen [12] who utilized the boundary value solution approach to the partial differential equation representation of a river with external thermal input. The resultant equations describe mathematically the average temperature distribution in a natural stream at every instant and at all points of the stream after the injection of a thermal pollutant. His ultimate goal was an accurate evaluation of a longitudinal heat dispersion coefficient that depends on bulk flow parameters and environmental factors.

The fourth broad category, that of time-series analysis of water temperature fluctuations, has been utilized recently to some extent by several authors. Since the bulk of the material which is presented in this dissertation falls into this category it is appropriate at this point to review some of the history of time-series analysis before discussing these more recent papers.

A presentation of time-series analysis is not complete without a discussion of the background of power spectral density techniques (see Appendix A). These techniques furnish one of the most powerful tools available to the time series analyst. The concept of a power spectrum has been utilized by the communications engineer for a number of years but its usefulness to other areas of application, such as weather data analysis, was not brought clearly into focus until the work of Blackman and Tukey [13] appeared in 1958. Other contributions to this subject were made by Tukey [14]

and Jenkins [15] in individual papers. In 1967 Parzen [16] edited a collection of papers, several of which were by Parzen himself, on time-series analysis. These papers included some excellent discussions on the use of power spectral density techniques in stochastic model building. An excellent text by Jenkins and Watts [17] was published in 1968. It gives a very detailed and rigorous treatment of power spectral density methods.

A very recent text by Jenkins and Box [18] concerns itself with the problems of forecasting and control of economic time-series analysis. The predictive modeling process is based on a technique which is referred to as the autoregressive moving average (ARMA) method. The analyses include the case where periodicities are present but very little discussion is devoted to power spectral density techniques.

Thus, power spectral density techniques are well documented and have seen wide application in various technical disciplines. In the area of hydrology, for example, Rodrequez-Iturbi [19] and Rodriquez-Iturbi and Nordin [20] have presented a detailed cross spectral analysis which shows the relative effect of rainfall, runoff, and dry bulb air temperature, respectively, on river water temperature. These results were informative but were only presented for the low-frequency range of one to six cycle/year. In this case monthly average water temperatures were used. Also, Roesner and Yevjevich [21] used power spectral density tech-

niques in the development of mathematical models for monthly precipitation and monthly water runoff. Again the frequency range of the calculations was limited to an upper frequency of six cycles/year because of the monthly sample interval.

The above papers are cited because they are direct examples of how power spectral density techniques can be used in the analysis of hydrological time-series data. However, they are limited to the particular applications discussed and do not answer many of the questions about the spectral content of river water temperature fluctuations. The reason for this is that the temperature spectral analyses which they have presented show only the effect of the very large yearly seasonal variation of water temperature. This effect, however, is immediately evident from a cursory examination of any time-series of daily average river water temperature. Thus, a major contribution of this dissertation is the extension of the power spectral density analysis to include the spectral effects of fluctuations which occur both at frequencies near the one cycle/year fluctuation and at higher frequencies up to at least 400 cycles/year.

In order to obtain the desired results at frequencies near the one cycle/year fluctuation, it was necessary to consider some means of extracting this very large cyclic component. To do this, a least-squares Fourier series fit to the time-series data was used. The one cycle/year Fourier approximation was then extracted by subtraction to yield a residual data set. The spectral content of this residual

data set was then analyzed to obtain useful information about low-frequency fluctuations in water temperature.

The theory of Fourier series has been well documented for many years. In general, however, it is applied to well defined periodic functions. The work of Chapman and Bartels [22] stands out as a classic treatise in the application of Fourier series techniques to the approximation of almost periodic (or nearly periodic) functions which occur in the area of geomagnetics.

For water temperature fluctuations, it was necessary to consider the fact that the data points exhibited a strong resemblance to a random process fluctuating about the nearly periodic yearly seasonal fluctuation. That is, it appeared to be of the form

$$X(t) = \overline{X} + C \cdot \sin (2\pi t + \phi_1) + n(t) \tag{2}$$

where

   $X(t)$ = river water temperature,

   $\overline{X}$ = average water temperature,

   C = peak amplitude of yearly seasonal fluctuation in water temperature,

   $n(t)$ = random fluctuations in water temperature, and

   ϕ_1 = initial phase angle.

Thus consideration had to be given to the Fourier series approximation in relation to the random process $n(t)$. As is shown in Appendix A, the Fourier series represents a least squares fit to discrete data points which contain random fluctuations.

In a very recent paper Kothandaraman [23] used this extraction technique in analyzing water temperature variations in a large river. His main objective was to build a regression model which would predict river water temperature by using a multiple regression model involving river water temperature and dry-bulb air temperature measurement. As a part of his model-building process he includes an analysis of the statistics of the water temperature residuals which are obtained when the first ten Fourier harmonics are extracted. He does not, however, include any reference to power spectral density techniques and does not justify his arbitrary extraction of the first ten harmonics. A part of this dissertation will be to demonstrate, with the aid of spectral analysis, that this extraction is valid with due caution being given to the fact that a portion of the spectrum which is extracted is actually random noise.

In addition to the power spectral density analysis, this dissertation gives consideration to the possibility of utilizing communication theory methods in the detection of thermal inputs to large rivers. Useful background information on communication theory was obtained from texts by Lee [24] and Hancock [25]. However, the most widely used texts on detection and estimation theory are those by Selin [26], Van Trees [27] and Helstrom [28]. These latter three texts, especially Van Trees, were used in the detection analysis. Useful information was also obtained from texts by Bendat and Piersol [29], and Robinson [30].

Further study of this problem indicated that, based on the above information, consideration should be given to the possibility of building a prediction model for river water temperature. This conclusion was based on the fact that an obvious criterion, which had already been taken into account by pollution control boards, was the setting of a maximum allowable increase in water temperature. Thus the prediction of above-normal water temperatures, particularly over the summer months, would be an invaluable aid to such agencies as well as to the power companies.

The following two chapters cover the principal results of the research which was outlined in the introduction and which has been formulated in more detail in this chapter. It was felt that the problem formulation should be presented as a part of the literature review since it was developed through a study of the background material which has been presented here.

III. POWER SPECTRAL DENSITY ANALYSIS

A. Introduction

The results presented in this section constitute the
first phase of a study to demonstrate the feasibility of
using communication theory techniques to establish a method
for estimating thermal pollution in large rivers. This
phase involves the calculation of the power spectral density
and subsequent spectral decomposition of water temperature
fluctuations which are based upon real-time temperature
records.

A portion of the temperature records used in this
analysis were made available through the courtesy of the
United States Geological Survey (U.S.G.S.) offices located
in Rolla, Missouri. The U.S.G.S. records cover time periods
of five years (1953 to 1958) and four years (1960 to 1964).
They consist of continuous strip chart temperature (°F)
recordings which were taken from the Missouri River at
Boonville, Missouri, by the U.S.G.S. The U.S.G.S. also made
available records of daily-average water temperatures which
had been tabulated from the continuous records.

Power spectral density calculations were made from both
the continuous and the daily average U.S.G.S. records. The
spectral calculations from the daily average records are
based on a sample interval of one day and hence a corresponding
Nyquist frequency range (see Appendix A) of 0 to 182.5
cycles/year.

The continuous records were sampled visually using a sample rate of four samples per day. This sample rate corresponds to a Nyquist frequency range of 0 to 730 cycles/year. Spectral plots are presented over this frequency range for the purpose of demonstrating the possibility of identifying thermal inputs on the basis of their cyclic properties.

One of the aims of this research was to obtain as much information as possible about the properties of the spectrum of temperatures of a large river. It was felt that the turbulence of the river might have a significant effect on water temperature because of the mixing of water at various temperature levels. The U.S.G.S. records were not accurate enough to allow a spectral analysis over the required frequency range. For this reason, additional temperature recordings were made in the Missouri River at Herrmann, Missouri, on June 10, 1971. The temperature readings which are used for the power spectral density calculations presented here were taken at 10 second sample intervals which correspond to a Nyquist frequency range of 0 to 360 cycles/hour.

The Herrmann temperatures, which were recorded in °C, were taken in the main channel of the river at eight-tenths of the channel depth. A frequency modulated quartz thermometer having a measurement resolution of .001° C at the 10 second sample interval was used.

B.   Methods of Analysis

1.   Fourier Series

Given that the bounded and continuous time-domain function, $f(t)$, is periodic with period T, then $f(t)$ can be written as:

$$f(t) = A_0 + 2 \sum_{k=1}^{\infty} [A_k \cdot \cos(\frac{2\pi kt}{T}) + B_k \cdot \sin(\frac{2\pi kt}{T})] \qquad (3)$$

where

$$A_0 = \frac{1}{T} \int_0^T f(t) \cdot dt, \qquad (4)$$

$$A_k = \frac{1}{T} \int_0^T f(t) \cdot \cos(\frac{2\pi kt}{T}) \cdot dt \qquad (5)$$

and

$$B_k = \frac{1}{T} \int_0^T f(t) \cdot \sin(\frac{2\pi kt}{T}) \cdot dt \qquad (6)$$

are the Fourier coefficients. If the period T is equal to one unit of time then the fundamental frequency is one cycle/(unit of time), and

$$f(t) = A_0 + 2 \sum_{k=1}^{\infty} [A_k \cdot \cos(2\pi kt) + B_k \cdot \sin(2\pi kt)]. \qquad (7)$$

For digital computer analysis, the time-domain temperature function $X(t)$ is sampled over one period, T = 1 year, to

obtain the time series $X(t_i)$, $i = 1, 2, \ldots, N$, where N is the number of sample points. The sampled versions of the corresponding Fourier coefficients (see Appendix A) are then

$$A_{os} = \frac{1}{N} \sum_{i=1}^{N} X(t_i) \tag{8}$$

$$= \bar{X},$$

$$A_{ks} = \frac{1}{N} \sum_{i=1}^{N} X(t_i) \cdot \cos(2\pi k t_i), \tag{9}$$

and

$$B_{ks} = \frac{1}{N} \sum_{i=1}^{N} X(t_i) \cdot \sin(2\pi k t_i). \tag{10}$$

2. Power Spectral Density

For the power spectral density calculations which are obtained in this analysis, $X(t_i)$ is first transformed to a zero-average time-series $X_o(t_i)$ where

$$X_o(t_i) = X(t_i) - \bar{X}. \tag{11}$$

The raw estimate, $\tilde{P}(f)$, of the true power spectral density for a given frequency, f, is taken as (see Appendix A)

$$\tilde{P}(f) = 2 \cdot \Delta t \cdot \{ \hat{R}_o + 2 \sum_{r=1}^{M-1} [\hat{R}_r \cdot \cos(\frac{\pi r f}{f_c})] + \hat{R}_M \cdot \cos(\frac{\pi M f}{f_c}) \} \tag{12}$$

where

Δt = time interval between samples,

f = frequency,

f_c = $1/2 \cdot \Delta t$; Nyquist frequency,

r = autocorrelation lag number,

M = maximum value of r,

and where $\hat{R}_r$ is the estimated autocorrelation function of $X_o(t_i)$. In this analysis, $\hat{R}_r$ is taken as (see Appendix A)

$$\hat{R}_r = \frac{1}{N - r} \sum_{i=1}^{N-r} X_i \, X_{i+r}; \quad r = 0, 1, \ldots, M \quad (13)$$

where M is the maximum value of the lag number r.

C. Results and Discussion

1. Low-Frequency Spectrum

The low-frequency spectrum will be defined as the discrete power spectral density of daily average river temperature for a frequency range of 0 to 182.5 cycles/year. This corresponds to a Nyquist folding frequency of 182.5 cycles/year for a one-day sample interval. Because the water temperature was averaged on a daily basis, the diurnal fluctuation and the high-frequency noise have been effectively filtered so that no high-frequency folding will occur. Also, the average temperature is extracted in order to avoid a very large spike at zero frequency.

Spectral calculations for the daily average data records showed that, for practical purposes, the power spectral content is concentrated in a frequency range which is much

smaller than the defined low-frequency range. For this reason, the low-frequency spectral plots will include only those frequencies where significant peaks have been found.

2. Spectra for Long-Term Records

Although the base frequency of one cycle/year was chosen for purposes of analysis, it was felt that useful information regarding long-term trends could be obtained by using data record lengths of longer duration than one year. The power spectral density for the five year (1953-1858) record is shown in Figure 1.

An obvious problem is encountered with regard to interpreting this power spectral density plot near one cycle/year. The extremely large spike corresponding to the yearly cyclic (or almost cyclic) variation in water temperature effectively masks the spectral contribution of neighboring frequencies. In order to extract this spike, a least-squares Fourier analysis was performed on the 1953-1958 data record. This analysis yielded a one cycle/year component having a peak amplitude of $24.9°$ F. A residual data record was then obtained by subtracting the one cycle/year Fourier approximation from the raw data.

A power spectral density analysis of this residual record produced the plot shown in Figure 2. This plot shows that some relatively strong cyclic fluctuations occur in the residual data at frequencies greater than one cycle/year. However, the most noticeable phenomenon is the occurrence of
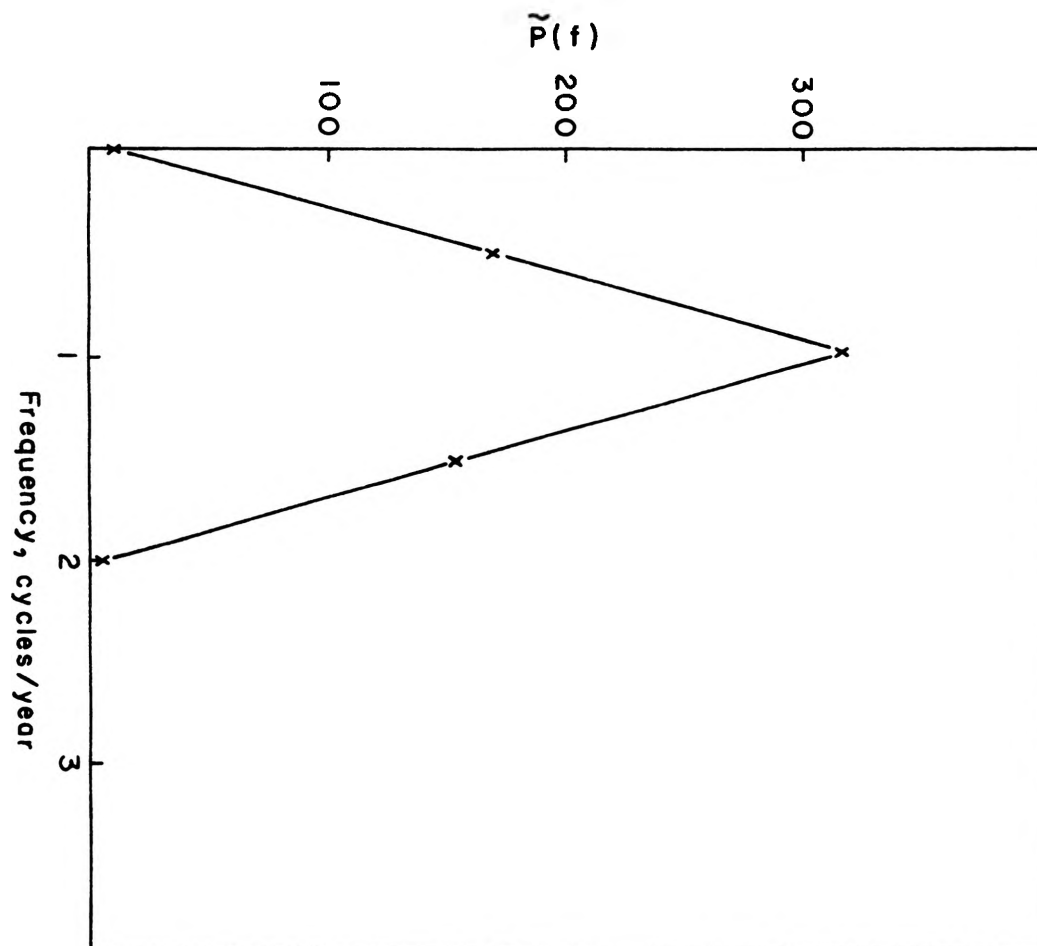
Figure 1.   Power Spectral Density for 1953-58 Data Record with $\overline{X}$ Removed.
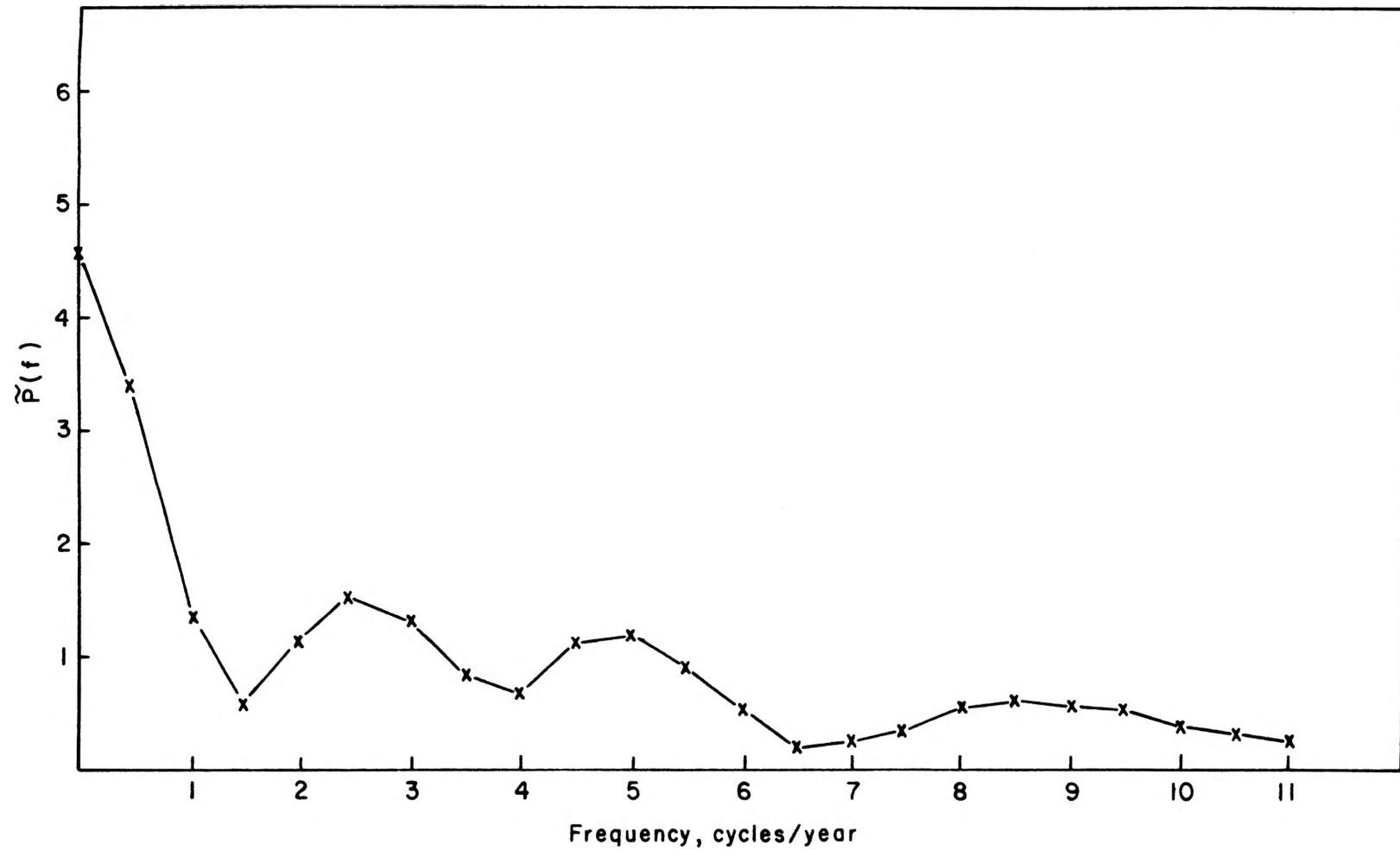
Figure 2. Power Spectral Density for 1953-58 Data Record with $\overline{X}$ and Fundamental Component Removed.

the high spectral strength in the frequency range between zero and one cycle/year. This is attributable to long-term fluctuations in the water temperature.

A comparison of the relative strength of these long-term fluctuations for different data segments can be made by the use of spectral plots similar to the one shown in Figure 2. As an example, Figure 3 shows spectral plots of the residual records for both the 1953-56 data segment and for the 1960-63 data segment. Note that only a three-year portion of the 1953-58 data record was taken since a valid comparison could be made only on the basis of equal record lengths. It is evident from these spectral plots that the long-term fluctuation (trend) in the 1953-56 data segment is greater than that for the 1960-63 record.

3. Spectra for One-Year Records

Because the yearly seasonal fluctuation of water temperature is predominant in the data record, a one year record length corresponding to the base frequency of one cycle/year was found to be the most convenient for purposes of analysis. At first, the data records were spectrally analyzed on a yearly basis. In each case, the fundamental (one cycle/year) component was removed prior to the spectral calculations.

The resulting power spectral density plots showed the existence of significant peaks at frequencies greater than one cycle/year. This was to be expected since the power spectral density for the long-term record had already
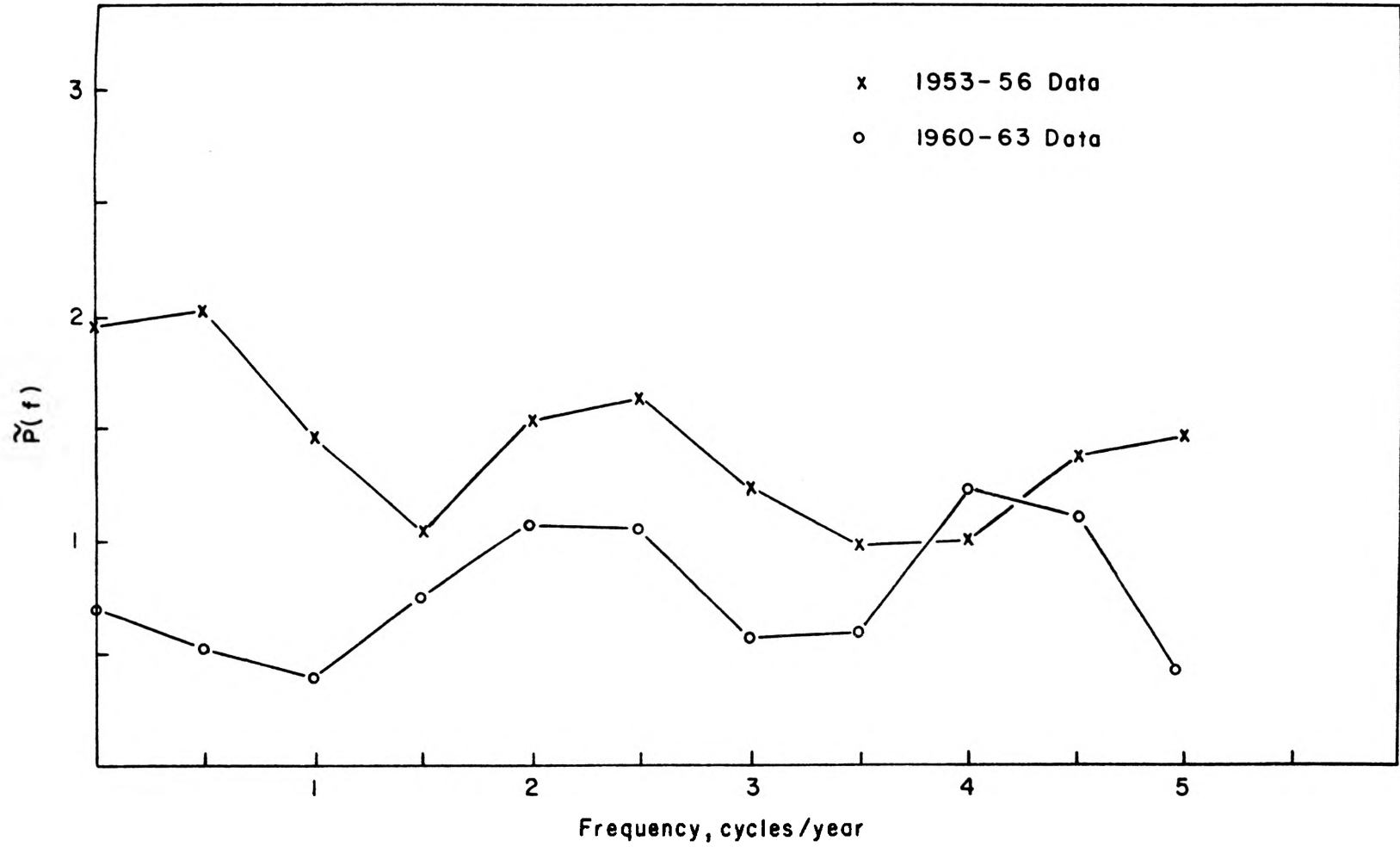
Figure 3.   Three-Year Power Spectral Density Records.

confirmed this. However, there was no consistency in the occurrence of these peaks from one year to another. This fact is illustrated in Figures 4 and 5. The power spectral density plot for 1960 is shown in Figure 4 while that for 1961 is shown in Figure 5. A significant peak occurs only at 2 cycles/year for the 1960 record while significant peaks occur at 2, 4, and 7 cycles/year for the 1961 record. Thus an attempt to build a predictive model would be completely inadequate if one year of data were used to predict temperatures for the following year.

In order to obtain a clearer understanding of the nature of the occurrence of these spectral peaks, a data shift having a time increment of 30 days was used instead of the one-year shift. This data shifting process involved

   (1)   calculation of power spectral density for data points 1 to 365,

   (2)   shifting the data record ahead by 30 days and calculating the power spectral density for data points 31 to 395,

   (3)   repeating step (2) until the entire data record was exhausted.

This 30-day increment was found to be sufficient to show the rise and subsequent decay of low-frequency spectral peaks. The 1960-64 data record was used for this part of the analysis.

For the first part of the 1960-64 data record the only significant spectral peak was at 2 cycles/year. Figure 6
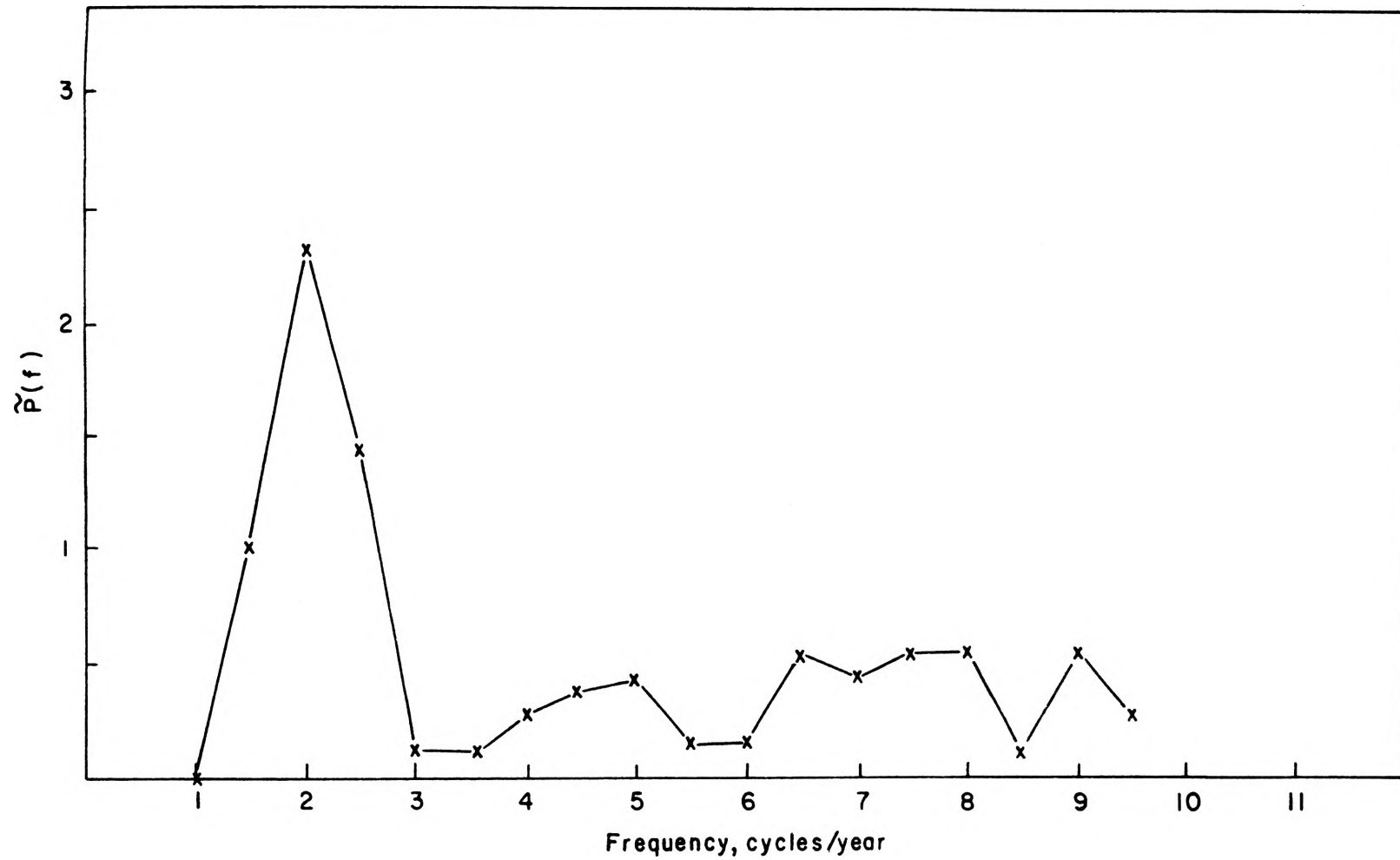
Figure 4. Power Spectral Density for 1960 Data Record with $\bar{X}$ and Fundamental Component Removed.
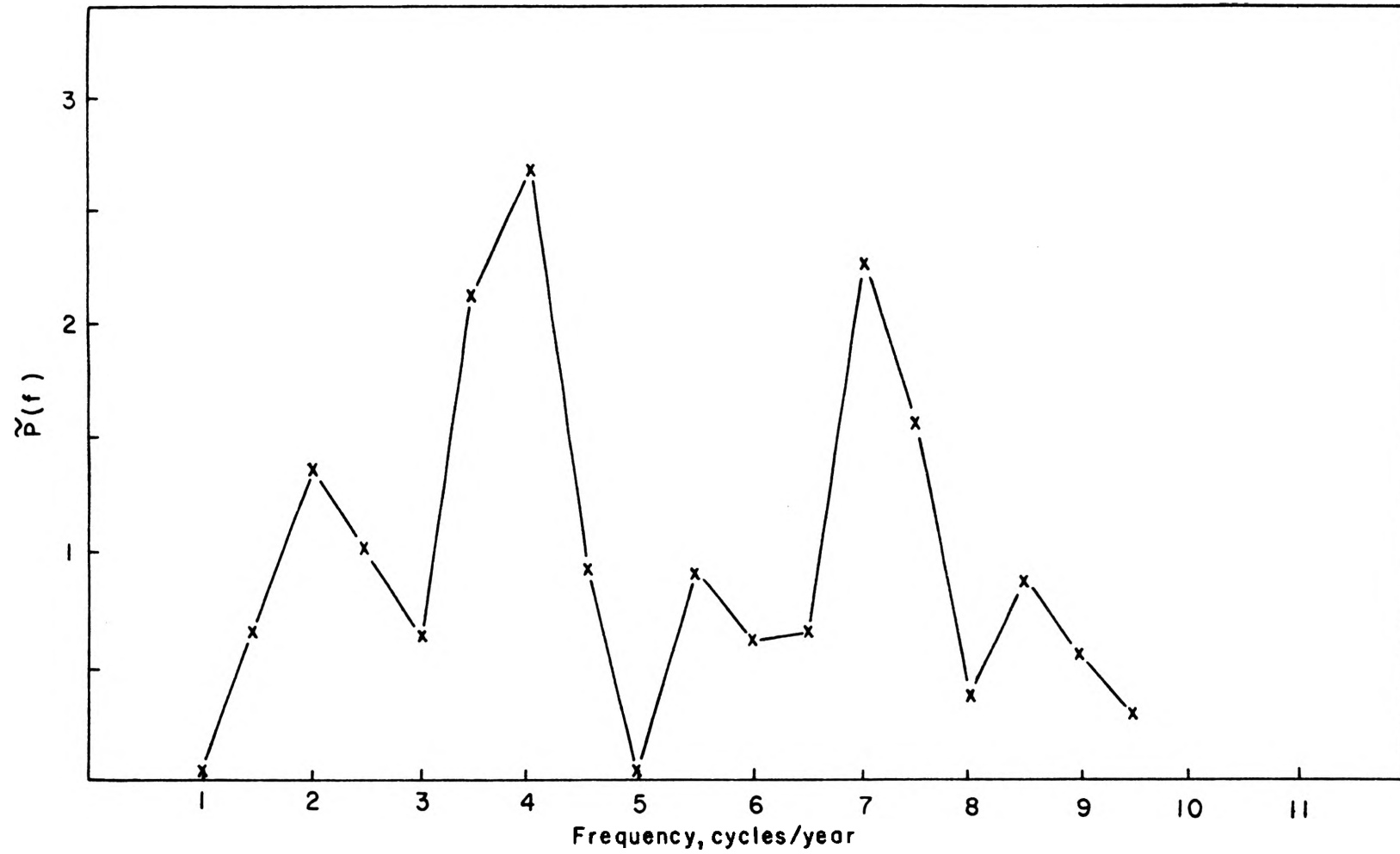
Figure 5. Power Spectral Density for 1961 Data Record with $\overline{X}$ and Fundamental Component Removed.

illustrates the spectral plots for this portion of the data record for three 30-day increments. The 2 cycle/year peak is seen to be in a state of decay.

Figure 7 shows a three-dimensional plot of power spectral density which is obtained by using a third axis on which to plot increment numbers. Three plots are shown, one for each of increments 7 through 11. These increment numbers were chosen so that the maximum value of the 4 cycles/year spectral peak occurs. The rise and decay effect demonstrated by this three-dimensional diagram was found to occur consistently in the spectral calculations.

These results suggest that a mathematical model of the river temperature would have to include this rise and decay effect. A particular frequency component, $s_k(t)$, having time-variable amplitude $C_k(t)$, is representable by the time-domain function

$$s_k(t) = C_k(t) \cdot \sin(2\pi kt + \phi_{ok}) \qquad (14)$$

where

t = time,

k = Fourier harmonic number, and

ϕ_{ok} = the initial phase.

A final point needs to be made in regard to the extraction of the harmonic components by the method of least-squares fit to the one-year data records. This concerns the validity of the extraction process itself. If, for example
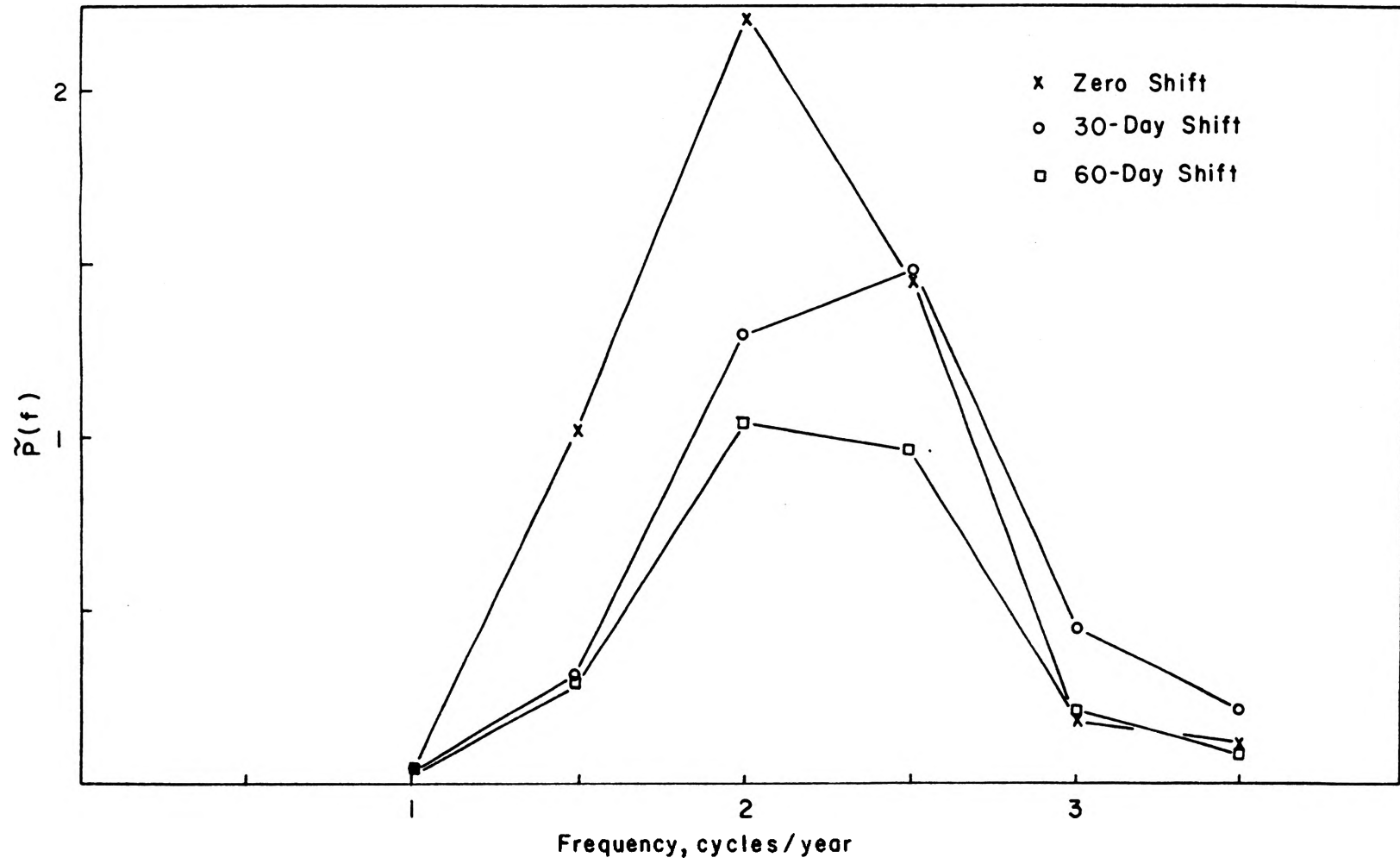
Figure 6.   Power Spectral Density Near 2 cycles/year for 1960 with $\overline{X}$ and Fundamental Component Removed.
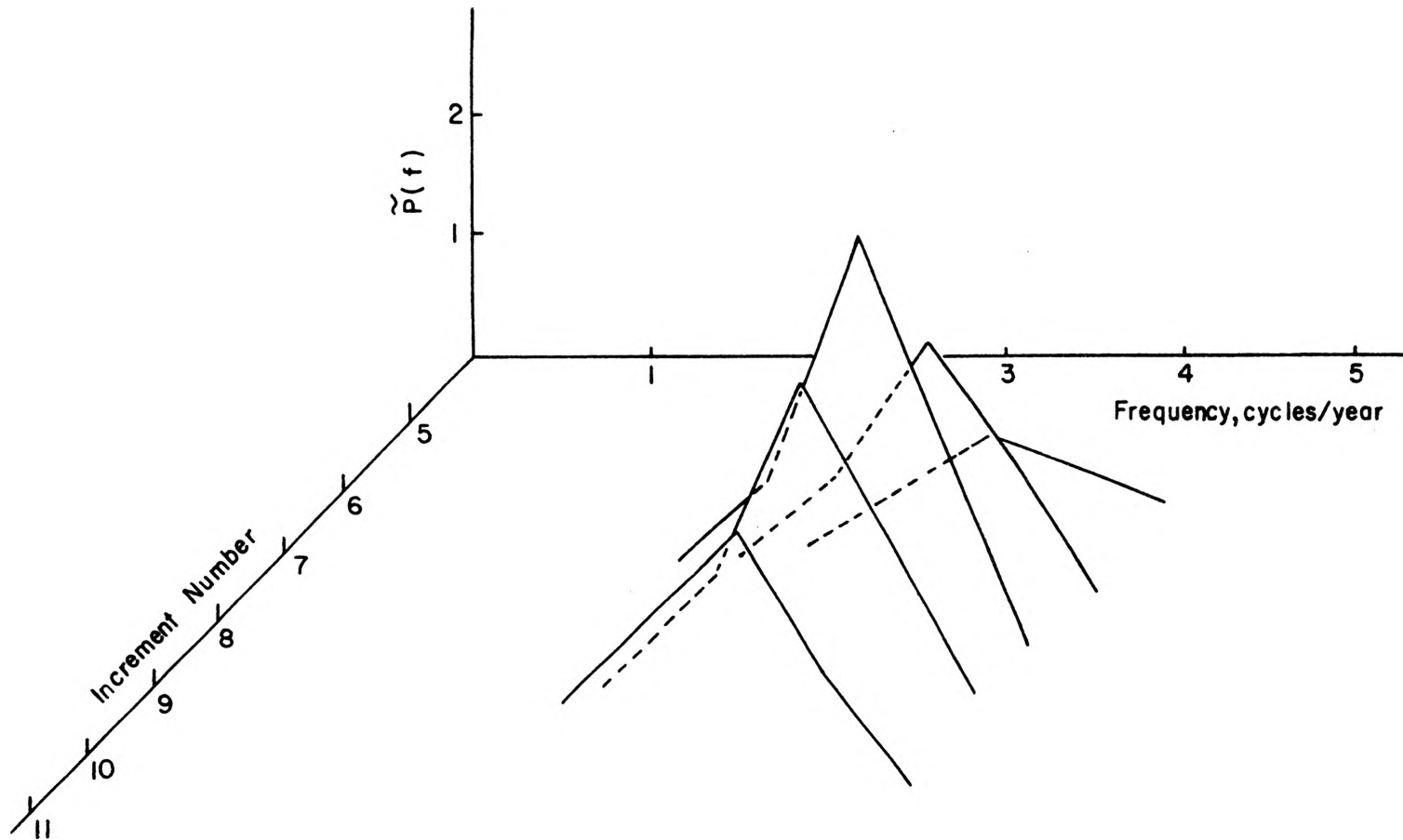
Figure 7. Incremented Power Spectral Density Plots for Portion of 1960-64 Data Record.

the spectral content of the data record is extracted for a given frequency range, then it should follow that the resulting spectral content would be negligible for the same range of frequencies. That this is true is demonstrated by Figure 8 which shows the resulting power spectral density plot for a typical one-year data record. In this case the Fourier components through the tenth harmonic were extracted. Correspondingly, the spectral density calculations, as shown in the graph, were insignificant for this same frequency range. Similar results were obtained for several of the residual records which were obtained for other data periods of one year. In this case, also, it should be pointed out that the spectral content at frequencies lower than one cycle/year is negligible because the record length is equal to the assumed fundamental period of one year. As mentioned previously, long-term fluctuations were very much in evidence when data segments of five years and four years were taken. In that case, however, no extraction at frequencies corresponding to those record lengths (1/5 cycle/year and 1/4 cycle/year) were made.

4. High Frequency Spectrum

The high-frequency portion of the spectrum of water temperature is defined as the frequency range 0 to 730 cycles/year. The 730 cycles/year Nyquist frequency corresponds to the four readings per day which were used to sample the continuous temperature recordings.
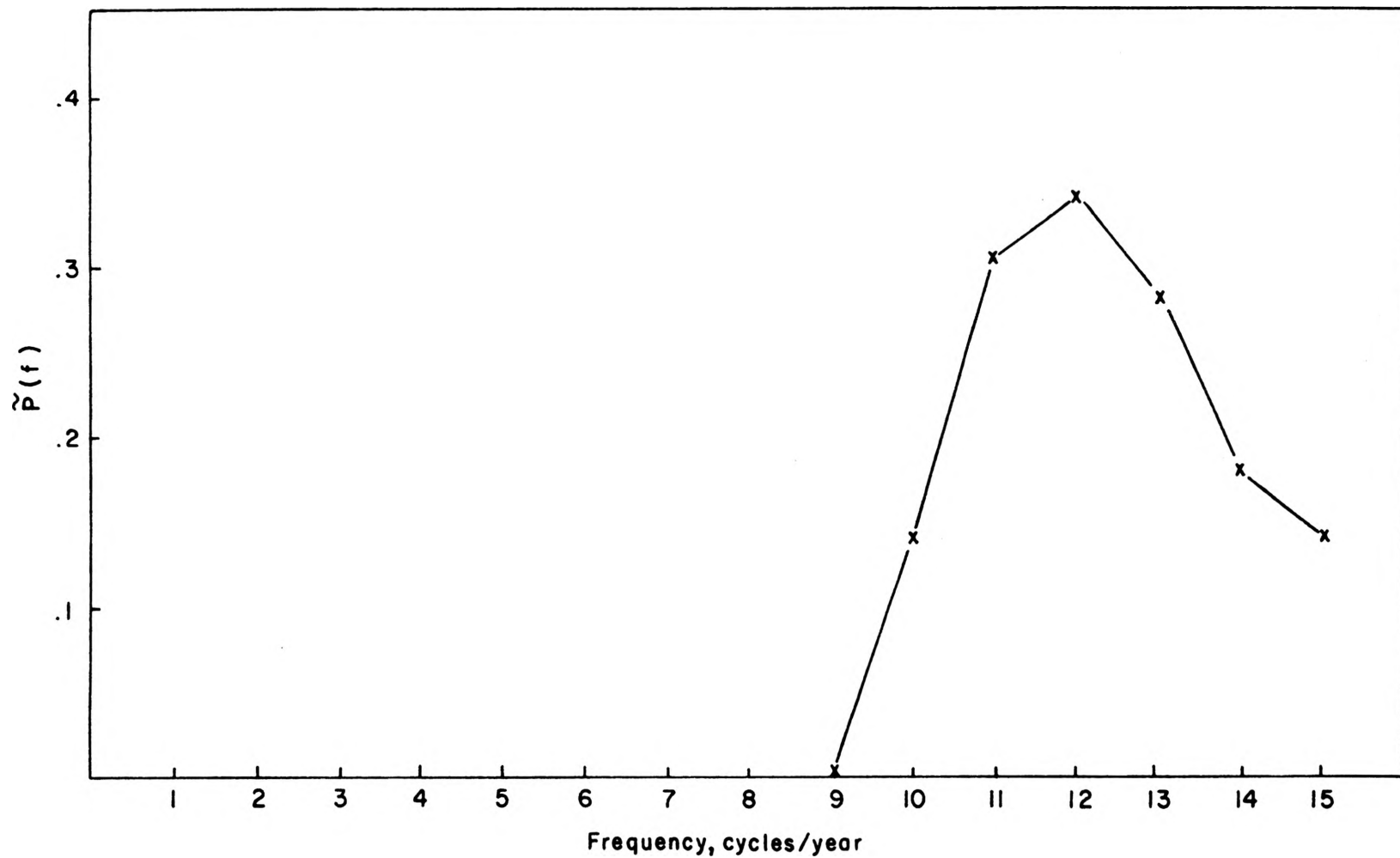
Figure 8. Power Spectral Density for 1953 Data Record with $\bar{X}$ and First Ten Harmonics Removed.

A one-year record length for the year 1964 was chosen for a first analysis. The large one cycle/year spike, as expected, dominated that portion of the spectrum near one cycle/year. Therefore, it was ignored in the plot of the spectral data. Further, because the frequency range covered was so broad, only the frequency ranges where noticeable peaks occurred were plotted.

The resultant spectral plot for the 1964 record is shown in Figure 9. The strong peak at 365 cycles/year is evidence of the diurnal fluctuations in the water temperature which were visually detectable on the continuous temperature record from which the samples were obtained. The 16, 30, and 52 cycle/year fluctuations, however, were not detectable by visual inspection of the continuous record.

Thus the power spectral density analysis definitely shows that cyclic fluctuations, which could not have been visually detected from the time-domain data alone, were present in 1964. The question arises, in particular, as to the cause of the 52 cycle/year fluctuation. A part of this study was to determine whether or not cyclic thermal pollutants could be detected by spectral analysis techniques. One preconceived notion was that a 52 cycle/year fluctuation might exist because of the weekly business cycle. In order to attempt to answer this question, the continuous record was sampled for the first year of record (1953).

The overall results of this analysis were similar to the 1964 results. Because most of the interest centered
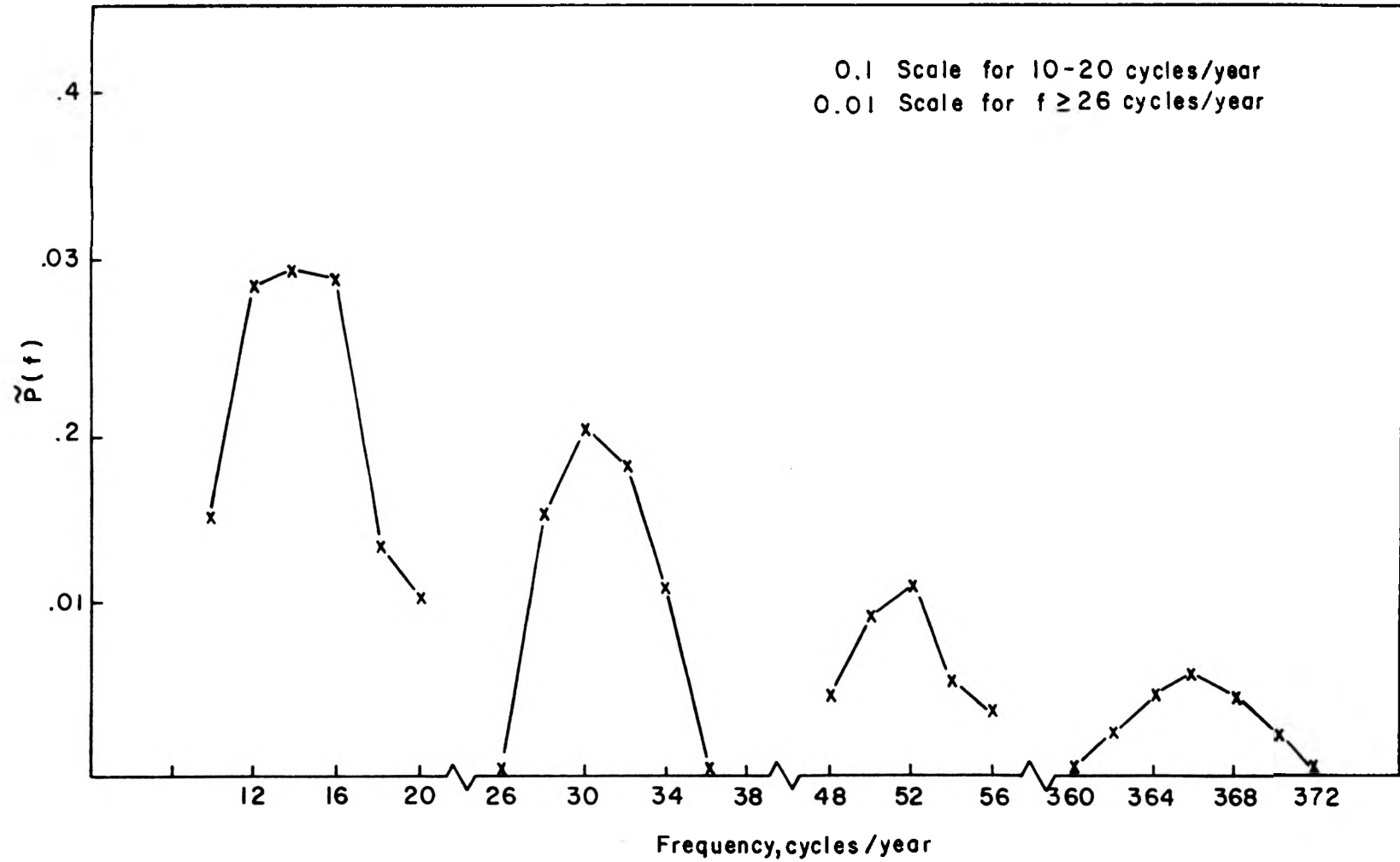
Figure 9.   Power Spectral Density for 1964 (4 samples/day).

around the 52 cycle/year fluctuation, only that portion of the spectrum was plotted for the 1953 record. The power spectral density plots in the neighborhood of 52 cycles/year for both the 1953 and the 1964 records are shown in Figure 10. A noticeable shift away from 52 cycles/year occurs for the 1953 record. In this case, the peak occurs in the 58 to 60 cycle/year frequency range. Also, the spectral-density level for the 1953 record is greater for a wider band of frequencies.

In an effort to determine the effect on the spectrum of a known 52 cycle/year fluctuation, a periodic test signal with period equal to one week was added to the 1964 sample record. This test signal consisted of a daily temperature increase of 0.1° F which lasted for 5.25 days. The test signal temperature was then dropped to 0° F for the remaining 1.75 days (corresponding to a weekend). The test signal was allowed to run for the duration of the 1964 data record. In Figure 11 the plot of the spectrum near 52 cycles/year (1964) is shown both with and without the test signal input.

No attempt has been made to place any significance on these 52 cycle/year fluctuations insofar as thermal pollution is concerned. In order to do this with any certainty, it would be necessary to have temperature records available for the time periods before the existence of power plants and cities on this river. The aim here is to demonstrate that power spectral density techniques are applicable in the detection of future changes in cyclic thermal properties of
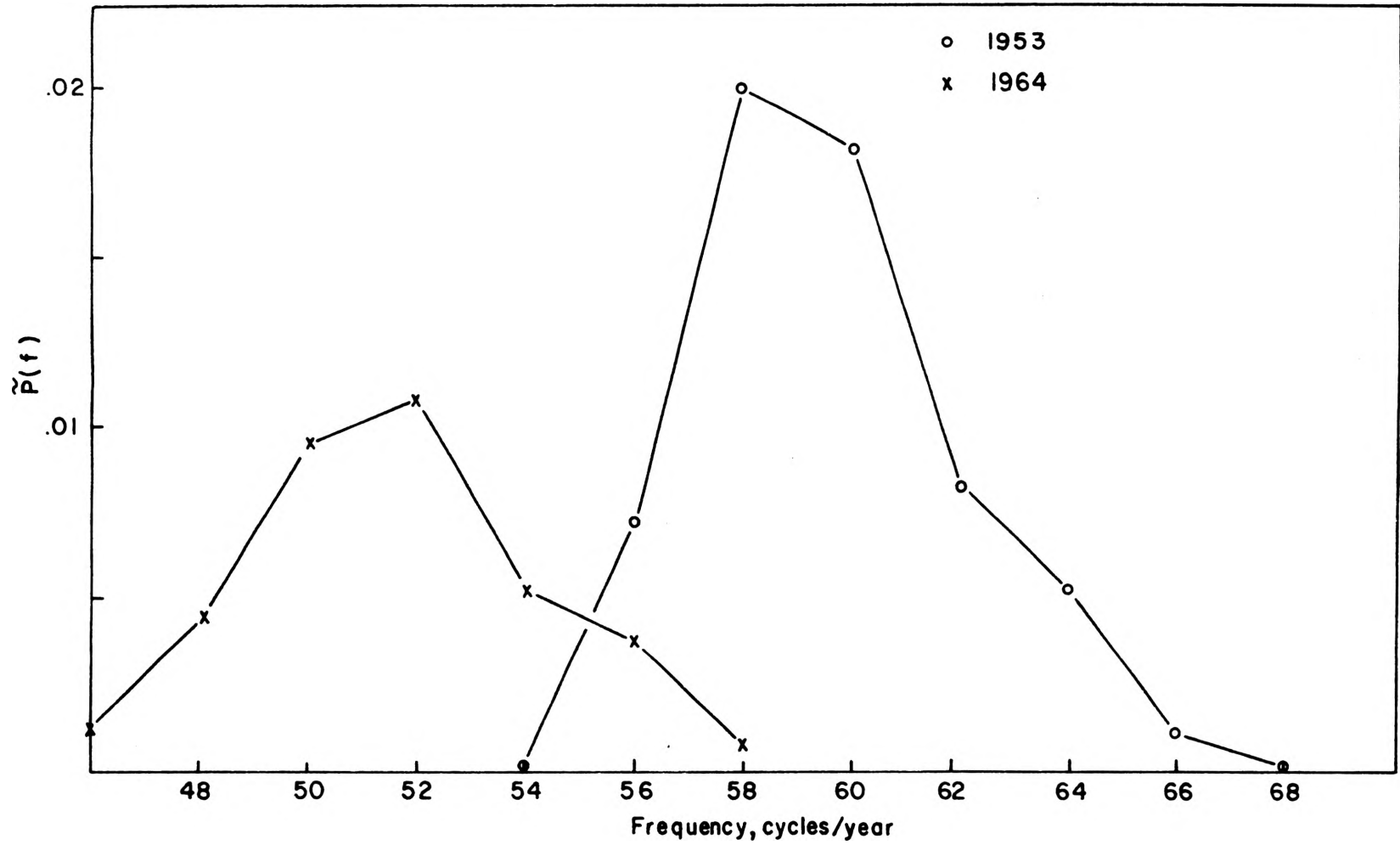
Figure 10. Power Spectral Density Plots for 1953 and 1964 (4 samples/day).
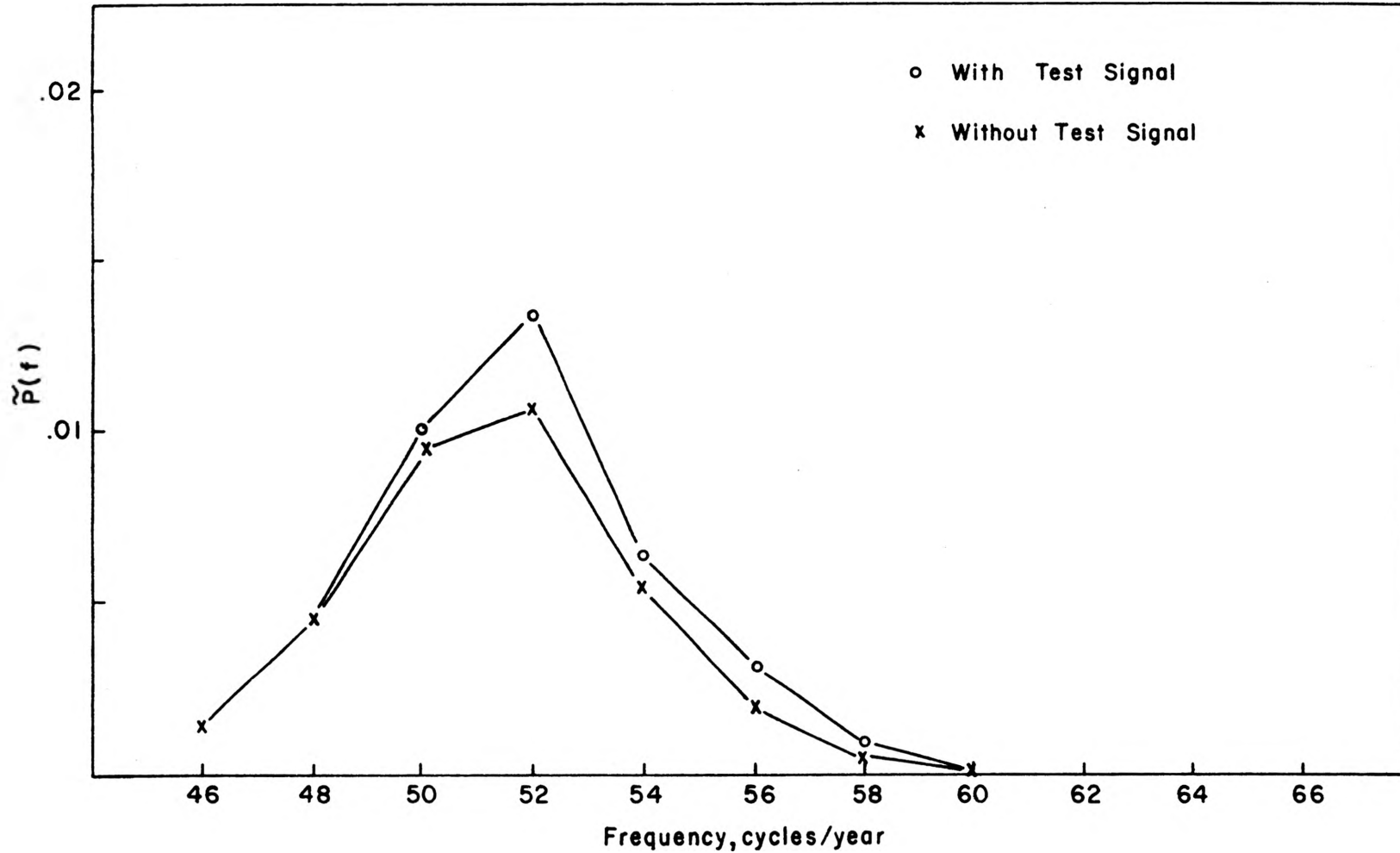
Figure 11. Power Spectral Density Plots for 1964 with and without Test Signal Input (4 samples/day).

our large rivers. Whether these changes are man-made or natural can only be decided after a thorough study of and comparison with the spectral properties of a man-produced thermal inputs to the particular river being studied.

5. Turbulence Noise

As a continuing part of this investigation, efforts were made to characterize, on a spectral basis, the high frequency noise of river water temperature which is caused primarily by turbulence. The continuous records did not have sufficient accuracy to warrant an attempt to use them for such purposes. Thus more data had to be collected.

Temperature measurements were made on the Missouri River at Herrmann, Missouri, on June 10, 1971. Sample records were taken at three different depths for each of three different stations across the river. The measurements were made from the highway bridge at Herrmann.

The time-series records, when plotted, exhibited pulse-type fluctuations which appeared to be closely related to the velocity of the water. Thus, some of the measurements which were taken away from the main channel showed only one or two pulses in a given time of record because of the low flow rate. The record taken in the main channel at 0.8 depth showed the most promise for a spectral analysis since it exhibited more pulses in the given time of record.

The resulting plot of the power spectral calculations for the above record is shown in Figure 12. It can be seen
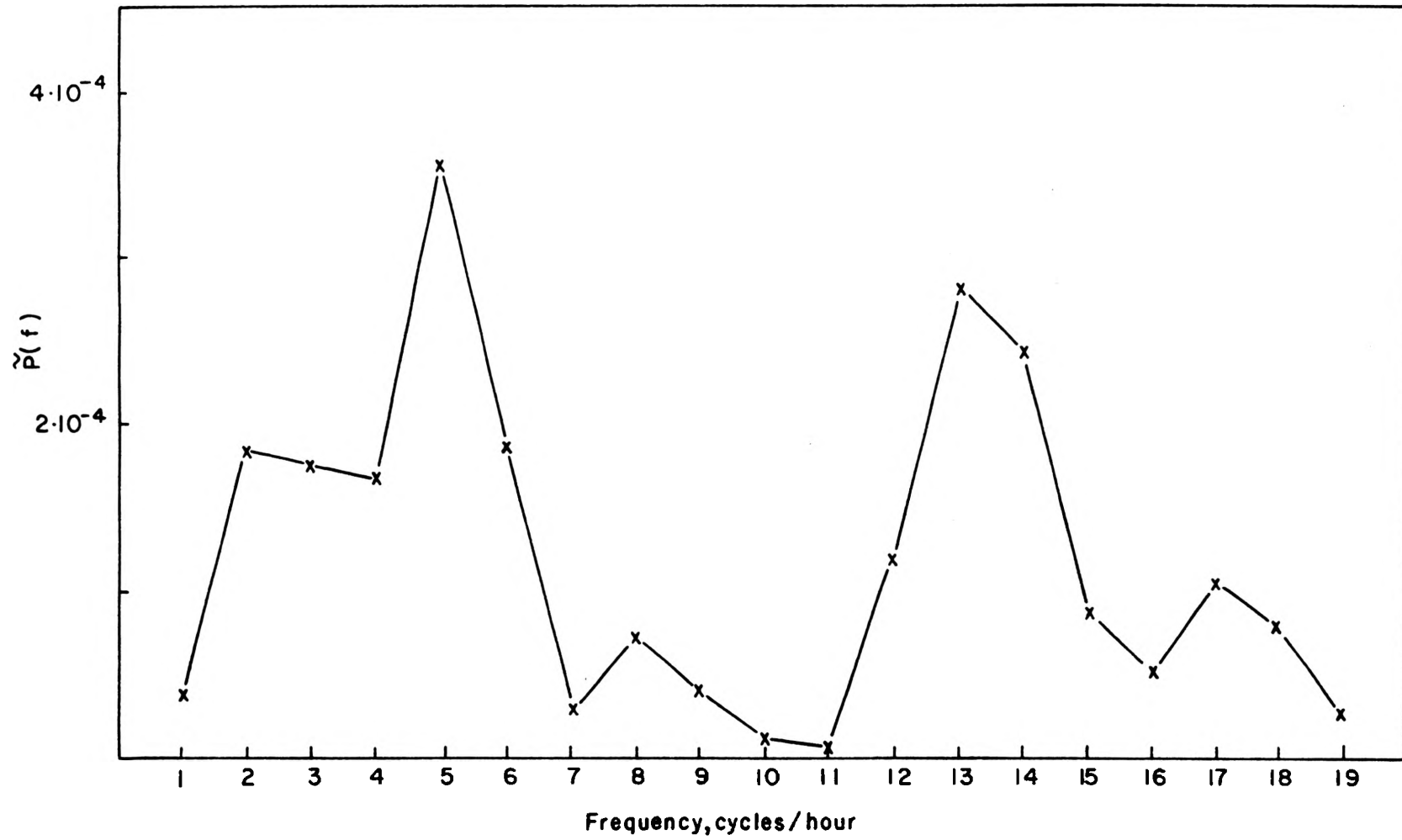
Figure 12. Power Spectral Density for Herrmann Data.

here that most of the high frequency noise is concentrated near 5 cycles/hour and near 15 cycles/hour. The 5 cycle/hour fluctuations correspond to the 20 minute record length while the 15 cycle/hour fluctuations correspond to the turbulence. Of course this only holds for this particular data record. Longer records are needed to better establish the spectral characteristics of this high frequency noise and, in particular, attempt to determine the relationship between spectral peaks and river flow rate.

IV. ESTIMATION AND PREDICTION

A. Introduction

Initial investigation of the long term records of the time-series for daily average water temperatures can be deceiving. The first impression is that a simple extraction of the one cycle/year component, along with the average temperature, over the record interval would leave a stationary random process with determinant statistical parameters. For example, one could analyze the residual record and test to see if it had normal distribution with μ and σ which could be estimated from the sample record. If this were true, then the problem of estimating thermal input levels would be a relatively simple process.

As seen from the power spectral density analysis, however, the problem is far from being simple. Even if the seasonal fluctuation actually did consist of a true sinusoid plus random noise, the problem would not be solved because of the long-term fluctuations which were discussed previously.

In considering these difficulties with regard to the estimation problem, it was decided that a better approach might be that of temperature prediction rather than estimation of thermal input levels. Thus, even though the estimation process is discussed and analyzed, emphasis is placed on the development of the prediction model.

It is shown that daily-average water temperature can be reliably predicted over at least a 60 day range. The

prediction range chosen covers a segment of the summer of 1962. This segment was chosen because the summer water temperatures are the most critical in regard to a maximum allowable water temperature which might be imposed by a water quality control board. Also, available time-series records show that the water temperature fluctuations are much larger during the warmer months of the year. Thus, a model which gives good prediction results during the summer months presumably would be at least as good a predictor during the winter months.

B. Fourier Regression Analysis

Observation of the time series $X(t_i)$, i = 1, 2, ..., N, which represents the daily average values of water temperature, clearly shows the predominance of a large annual cyclic variation. Thus, a separation of the data into its cyclic components by means of Fourier series is essential to the regression analysis process.

By taking one year of data, $X(t_i)$, i = 1, 2, ..., 365, and assuming a periodic extension of this particular record, we can write, for Fourier components one through n,

$$X(t_i) \cong A_{os} + 2 \sum_{k=1}^{n} [A_{ks} \cdot \cos(2\pi k t_i) + B_{ks} \cdot \sin(2\pi k t_i)] \quad (15)$$

where

$$A_{os} = \frac{1}{365} \sum_{i=1}^{365} X(t_i) \tag{16}$$

$$= \bar{X} ,$$

$$A_{ks} = \frac{1}{365} \sum_{i=1}^{365} X(t_i) \cdot \cos(2\pi k t_i), \tag{17}$$

and

$$B_{ks} = \frac{1}{365} \sum_{i=1}^{365} X(t_i) \cdot \sin(2\pi k t_i). \tag{18}$$

Note in these expressions that a base period of one year
$(T = 1)$ is again assumed so that the corresponding fundamental
frequency is one cycle/year. Because the sampled version of
the Fourier coefficients, A_{os}, A_{ks} and B_{ks}, are themselves
obtained by a least squares fit of the data to the kth
harmonic component, (see Appendix A), the least squares
approximation to the data is given by the finite series of
equation (15).

Thus, the desired regression equation is

$$F(t_i) = A_{os} + 2 \sum_{k=1}^{n} [A_{ks} \cdot \cos(2\pi k t_i) + B_{ks} \cdot \sin(2\pi k t_i)] \tag{19}$$

so that

$$X(t_i) \cong F(t_i). \tag{20}$$

For later use it will be more convenient to employ the alter-
nate form for $F(t_i)$ given by

$$F(t_i) = A_{os} + 2 \sum_{k=1}^{n} C_k \cdot \sin(2\pi k t_i + \phi_k) \qquad (21)$$

where

$$C_k = \sqrt{A_k^2 + B_k^2} \qquad (22)$$

and

$$\phi_k = \arctan \frac{A_k}{B_k} . \qquad (23)$$

The residual record defined by the difference

$$D(t_i) = X(t_i) - F(t_i) \qquad (24)$$

is used in analyzing the closeness of fit of the regression equation. By the use of power spectral density techniques it has been shown that the spectral content of $D(t_i)$ is insignificant for frequencies less than or equal to the maximum regression harmonic n. Thus, as $n \rightarrow \infty$, $D(t_i) \rightarrow 0$, $i = 1, 2, \ldots, 365$.

It is not practical, or even desirable, to allow the condition $n \rightarrow \infty$. The best approach seems to be a selection of n which allows the residual record to appear statistically as a normal random variable with mean zero over the one-year data interval. With this as a goal, the first complete year of record from the 1960-64 data set was analyzed.

This analysis consisted of selecting a value for n, obtaining the Fourier approximation, $F(t_i)$, and then performing a Kolmogorov-Smirnoff test on the residuals, $D(t_i)$.

Intermediate steps included calculation of both the standard error of estimate given by

$$\sigma_E = \sum_{i=1}^{365} \sqrt{[D(t_i)]^2/365} \tag{25}$$

as well as the probabilities necessary to allow a plot of the corresponding histogram. All residual sets for n = 1, 2, . . ., 10 satisfied the Kolmogorov-Smirnoff test for normal random processes with zero mean.

The graphical plot in Figure 13 illustrates the fit of the regression equation $F(t_i)$ for the value n = 1. For purposes of comparison, a plot of $X(t_i)$ is included in Figure 13.

C. Estimation of Thermal Input

In order to demonstrate how this regression model applies to the estimation process we consider a typical situation which is encountered in the thermal input process as applied to large rivers. This is illustrated in Figure 14 where X(t) represents the continuous version of the natural fluctuations in water temperature, while U(t) represents the thermal input. The combination of mixing and heat loss causes the net water temperature to decay so that it eventually approaches the natural temperature of the river.

By analogy, the thermal system in Figure 14 is represented by the communication system shown in Figure 15. The detector input consists of an attenuated version, $U_a(t)$, of
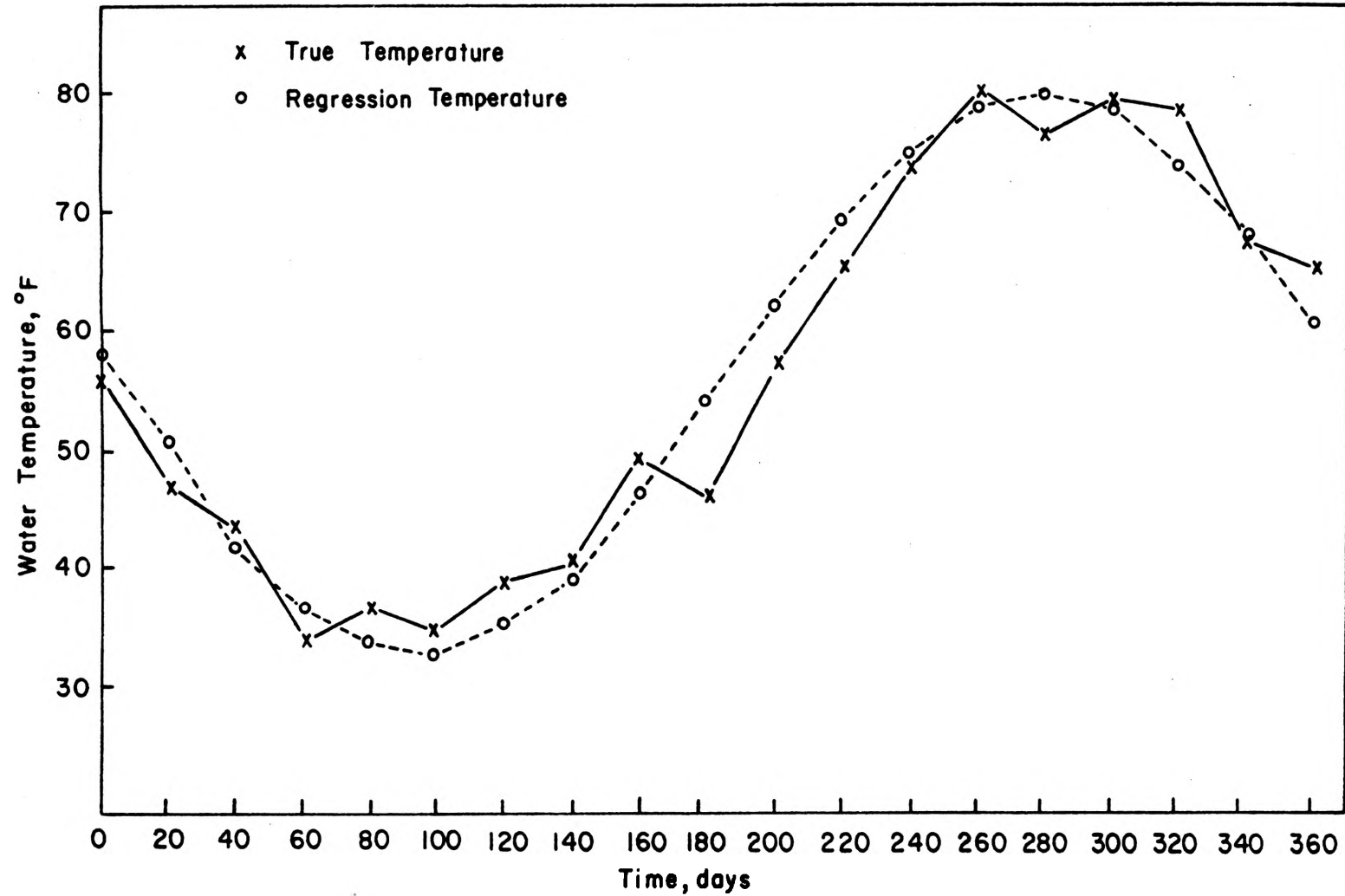
Figure 13. Fourier Regression Points and Daily Average Temperature, $X(t_i)$, for First
Year of 1960-64 Record.
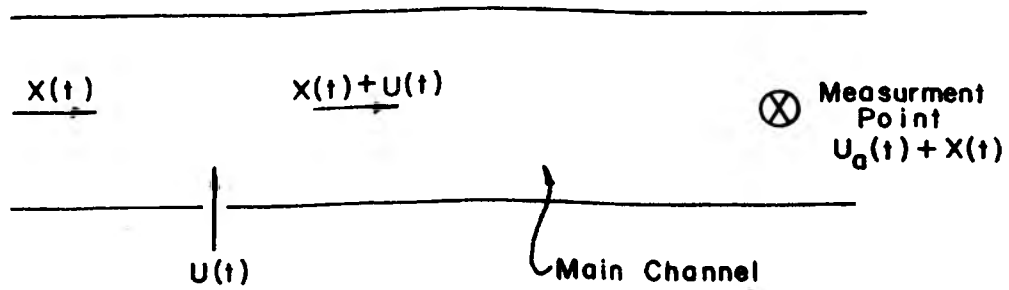
Figure 14. Assumed Thermal Process for Input to a Large River Channel.
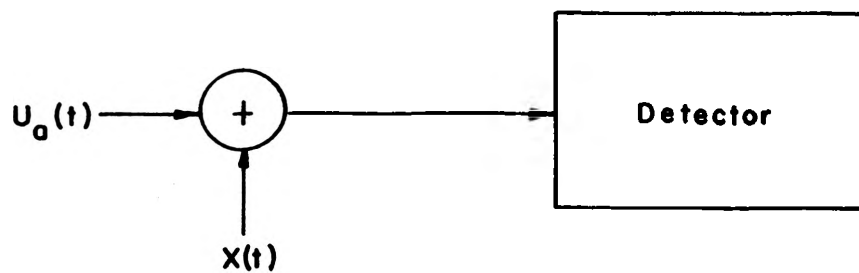
Figure 15. Communication System Analog of Thermal Process for Input to a Large River Channel.

U(t) along with X(t). This situation is illustrated by the block diagram in Figure 15. In this case, the detector must make the best estimate of $U_a(t)$ based on a measurement of signal plus noise represented by the sum $U_a(t) + X(t)$. Thus, for purposes of analysis, X(t) is the noise background from which the signal, $U_a(t)$, must be estimated.

As an example, assume that $U_a(t)$ is a fixed constant U_o. This would be representative of the thermal output of a power plant having a constant load demand. The input to the detector under this assumption is $U_o + X(t)$.

Since the daily average data record is conveniently available in tabular form, it is used in place of X(t). Thus for one year of record the detector must estimate U_o based upon an input of $U_o + X(t_i)$. Recalling from the regression analysis that $X(t_i)$ is representable in the form

$$X(t_i) = F(t_i) + D(t_i), \tag{26}$$

we write the input to the detector, $S(t_i)$, as

$$S(t_i) = U_o + F(t_i) + D(t_i) \tag{27}$$

$$= U_o + A_{os} + 2 \sum_{k=1}^{n} C_{ks} \cdot \sin(2\pi k t_i + \phi_k) + D(t_i)$$

The average value of $S(t_i)$ over one year of record is then

$$\overline{S(t_i)} = U_o + A_{os} + 2 \sum_{k=1}^{n} C_{ks} \cdot \sin(2\pi k t + \phi_k) + D(t_i) \tag{28}$$

$$\overline{= U_o} + \overline{A_{os}} + \overline{2 \sum_{k=1}^{n} C_{ks} \cdot \sin(2\pi kt + \phi_k)} + \overline{D(t_i)}$$

$$= U_o + A_{os} + \overline{D(t_i)} \; .$$

From the regression analysis $\overline{D(t_i)} \cong 0$ for sufficiently long data records so that

$$\overline{S(t_i)} \cong U_o + A_{os} \; . \tag{29}$$

Hence, if A_o is known, then

$$U_o \cong \overline{S(t_i)} - A_{os} \tag{30}$$

is a valid estimate of the thermal input U_o.

The assumption that A_{os} is known is an oversimplification since A_{os} can change radically from one year to another. This fact is well demonstrated in Figure 16 which shows a plot of values of $\overline{X} = A_{os}$ obtained by the moving average method using 30 day increments. The entire data record of daily average temperatures was used but only the 1960-64 portion of the record is plotted. These moving averages were found to vary over a temperature range of 55.6 °F to 58.6 °F for the 1960-64 data set and 55.3° to 60.8° for the 1953-58 set.

The difficulty here arises from the fact that a periodic extension of $X(t_i)$ was assumed in the original Fourier series expression for this time series. That is, the assumption $X(t + m) = X(t)$ for $m = \pm 1, \pm 2, \pm 3, \ldots$, is not true for
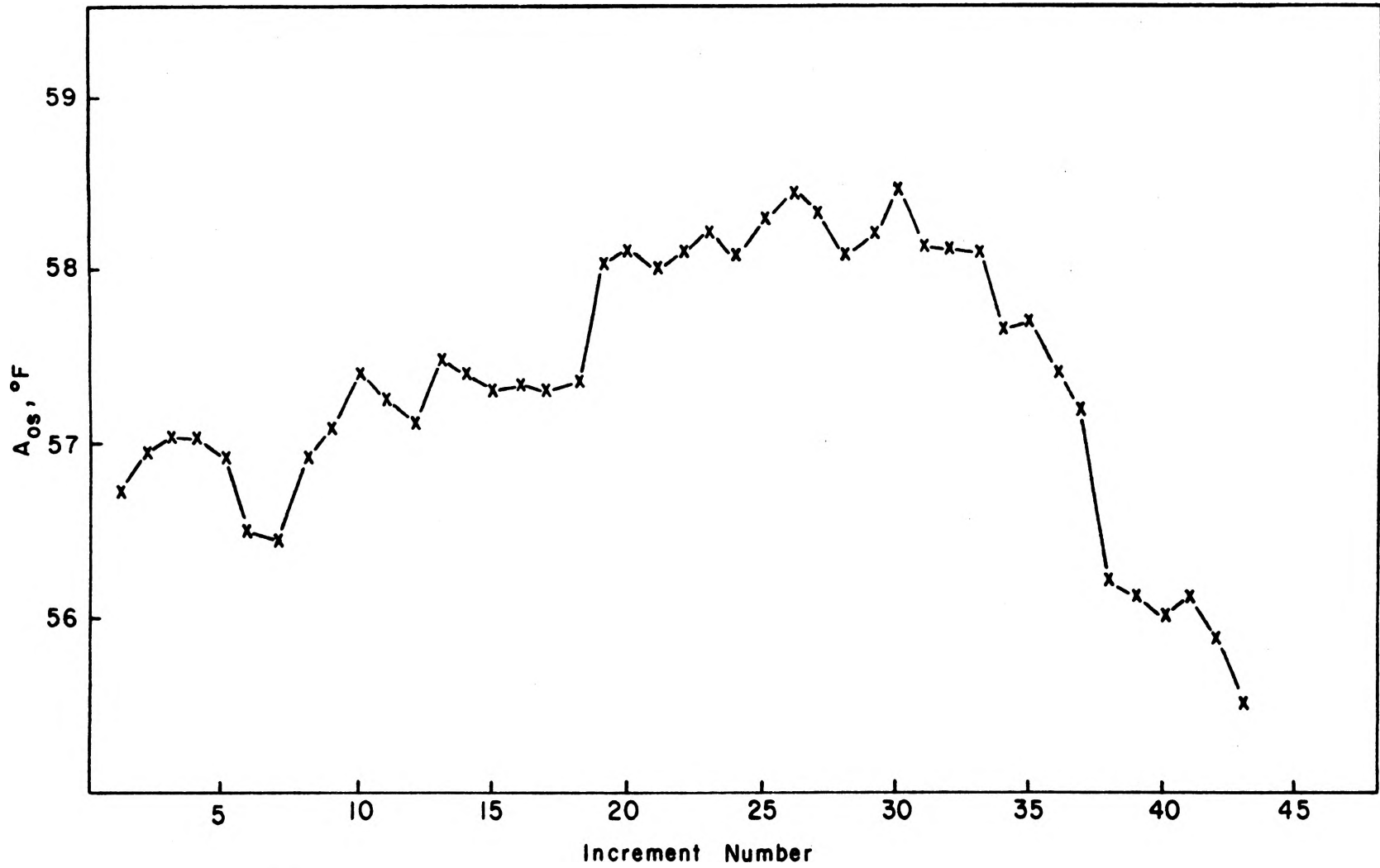
Figure 16. Moving Averages for A_{os} = $\overline{X}$ for 1960-64 Record.

the time series being studies. It should be noted, however, that for the constant thermal input, U_o, the Fourier components will always have zero average value for a one year data record. Hence the difficulty which arises in the estimation of U_o is that it is imbedded in the residual noise $A_{os} + D(t_i)$ which remains when the cyclic components are extracted.

Because $D(t_i)$ is a set of normal random numbers with mean zero, it follows that $A_{os} + D(t_i)$ for time periods greater than one year is equivalent to a set of normal random numbers with a very slowly fluctuating mean of A_{os}. It can be shown (see Appendix A) that the best statistical estimate of a constant signal in a normal random noise process with zero mean is just the statistic $\overline{X} = \frac{1}{N} \sum_{i=1}^{N} x_i$. Hence, if A_{os} were fixed, as in a truly periodic function, then A_{os} could be extracted along with the cyclic components so that the best estimate of U_o would be simply $\hat{U}_o = \frac{1}{365} \sum_{i=1}^{365} [U_o + D(t_i)]$. This would be identical to the value which would be obtained by the use of $U_o \cong \overline{S(t_i)} - A_{os}$.

It follows from the above discussion that in order to make a decision regarding the estimate of the thermal input U_o for a given year, some method of judgement regarding the value of A_{os} must be determined. One could conceivably use the average of the moving averages as an estimate of A_{os}. A more promising approach is to perform a polynomial regression on the moving averages of A_{os} and use an extrapolation curve to predict what the value of A_{os} should be for a predetermined time span. This predicted value of A_{os} could then be

subtracted from $\overline{S(t_i)}$ to obtain an estimate of U_o. This approach will be discussed again in the next section.

D. Forecasting of Water Temperatures

A more interesting and perhaps much more useful approach to the thermal input problem involves the forecasting or prediction of water temperatures. The following analysis demonstrates that the daily average water temperatures of large rivers can be accurately forecast for a prediction range of at least 60 days. The approach used in the analysis was prompted by the fluctuations in the moving averages of the yearly average water temperature, A_{os}, which were discussed in the preceding section.

The power spectral density calculations for one year data records of the time-series $X(t_i)$, which were discussed in Chapter II, are indicative of similar moving average variations in the Fourier component amplitudes, C_k, k = 1, 2, . . ., n. Verification of these variations was obtained by taking the moving average values using 30 day increments over a 360 day period for harmonic components one through ten. The first two-year segment of the 1960-64 data set was used for these calculations.

The variations in the Fourier components suggest that a representation of $X(t)$ having the form

$$X(t) = A_o(t) + 2 \sum_{k=1}^{\infty} C_k(t) \cdot \sin(2\pi kt + \phi_k) \tag{31}$$

where

$A_o(t)$ = slowly fluctuating yearly average of water temperature, and

$C_k(t)$ = slowly fluctuating Fourier component amplitude,

might be appropriate. This representation allows the prediction of $A_o(t)$, $C_k(t)$, $k = 1, 2, \ldots, n$, based on a polynomial regression approximation to the moving averages. The resulting temperature prediction equation then takes the form:

$$X_p(t_i) = A_{op} + 2 \sum_{k=1}^{n} C_{kp} \cdot \sin(2\pi k t_i + \phi_k) \qquad (32)$$

Note that A_{op} and C_{kp}, $k = 1, 2, \ldots, n$, are not written as time functions because they represent Fourier components which should, by prediction, remain fixed for a 365 day data period. This 365 day period represents, assuming data are available, data segments which would be used to obtain predicted moving average values for 10, 30, and 60 day shifts from the last regression data point. Thus the first 355, 335, and 305 days, respectively, calculated from the expression for $X_p(t_i)$ represent temperatures which are already known from measured values of $X(t_i)$. The predicted temperatures are then, respectively, the last 10, 30, and 60 day segments of $X_p(t_i)$.

For prediction of the Fourier components A_o, C_1, C_2 and C_4, a regression polynomial of the form $y = a + bx + \varepsilon$ was fitted to a 90-day data segment (nine 10-day moving average

increments). The initial point used in the calculations was obtained by shifting 150 days ahead of the first data point of the 1960-64 data set. This was done to allow prediction across the summer months because the summer water temperatures are the most critical. The results of this regression analysis are summarized in Table I and illustrated graphically in Figures 17, 18, 19, and 20.

It should be noted here that, as mentioned in the previous section, A_{op} might be used to obtain an estimate of the constant thermal input U_o. This estimate would take the form

$$\hat{U}_o = \overline{S(t_i)} - A_{op} \tag{33}$$

An initial effort in the forecasting of temperatures by $X_p(t_i)$ was made using only predicted values of A_o and C_1. The corresponding prediction equation was of the form

$$X_{p1}(t_i) = A_{op} + C_{1p} \cdot \sin(2\pi t_i + \phi_1) \tag{34}$$

The values of A_{op} and C_{1p} were obtained from the regression formulas, as illustrated in Figures 17 and 18, for 10, 30, and 60 day prediction ranges. The phase angle, ϕ_1, was obtained by using the calculated phase angle, ϕ_{01}, corresponding to the last regression data point and letting

$$\phi_1 = \phi_{01} + 2\pi \Delta t_p \tag{35}$$

where

TABLE I

SUMMARY OF REGRESSION DATA FOR REGRESSION RANGES
INDICATED IN FIGURES 17, 18, 19, AND 20.

Fourier Component	a, °F	b, °F	Maximum Error $y - \hat{y}$, °F	Standard Error of Estimate, °F
A_o	56.26	0.051	0.35	0.22
C_1	11.71	0.035	0.08	0.05
C_2	0.48	0.0055	-0.13	0.08
C_4	0.28	0.091	0.18	0.10

Figure 17. 90-day Regression Data Segment for A_{os} (Moving Average) with Prediction Line and Extended Extrapolation Line.
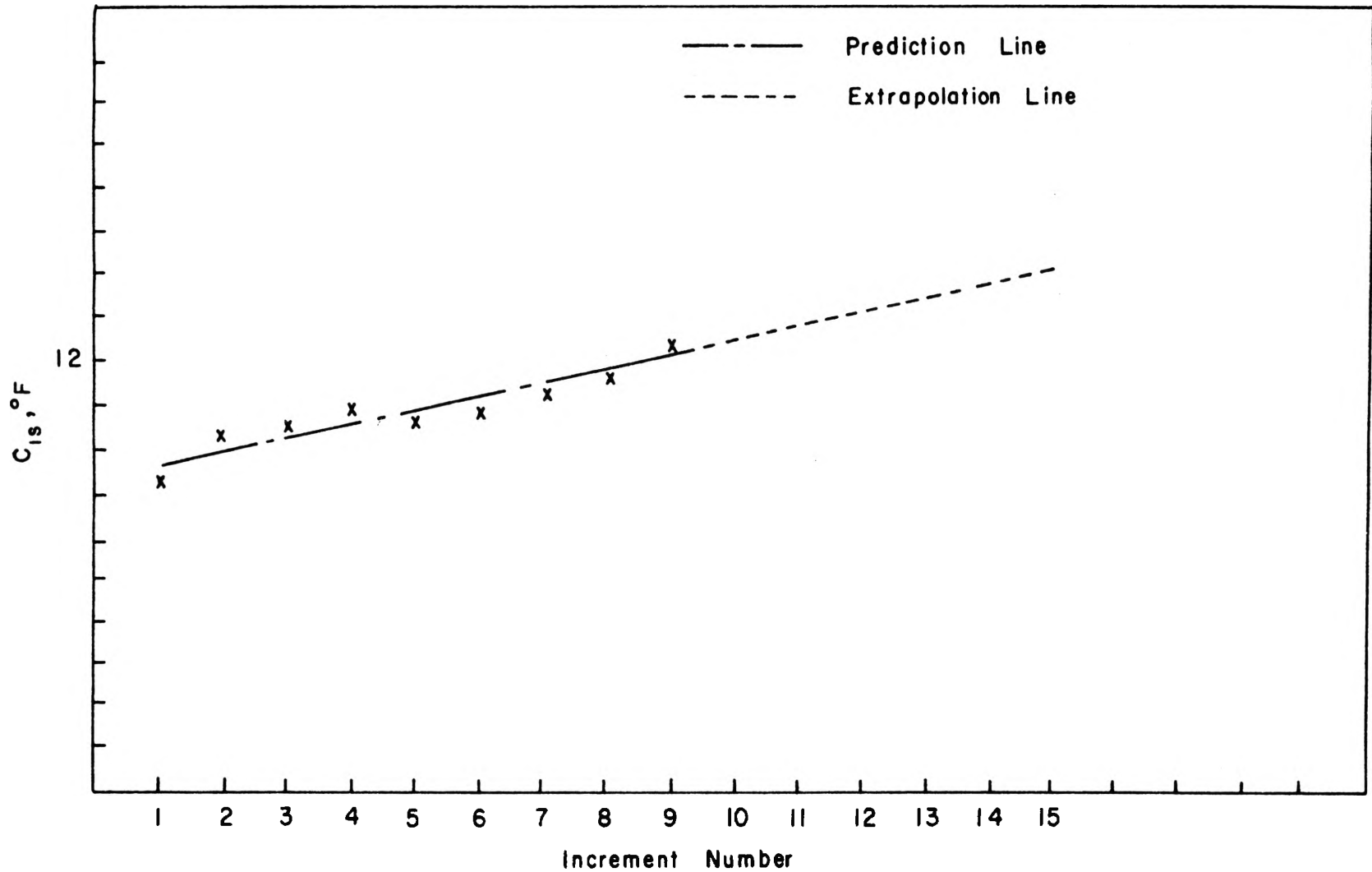
Figure 18. 90-day Regression Data Segment for C_{1s} (Moving Average) with Prediction Line and Extended Extrapolation Line.
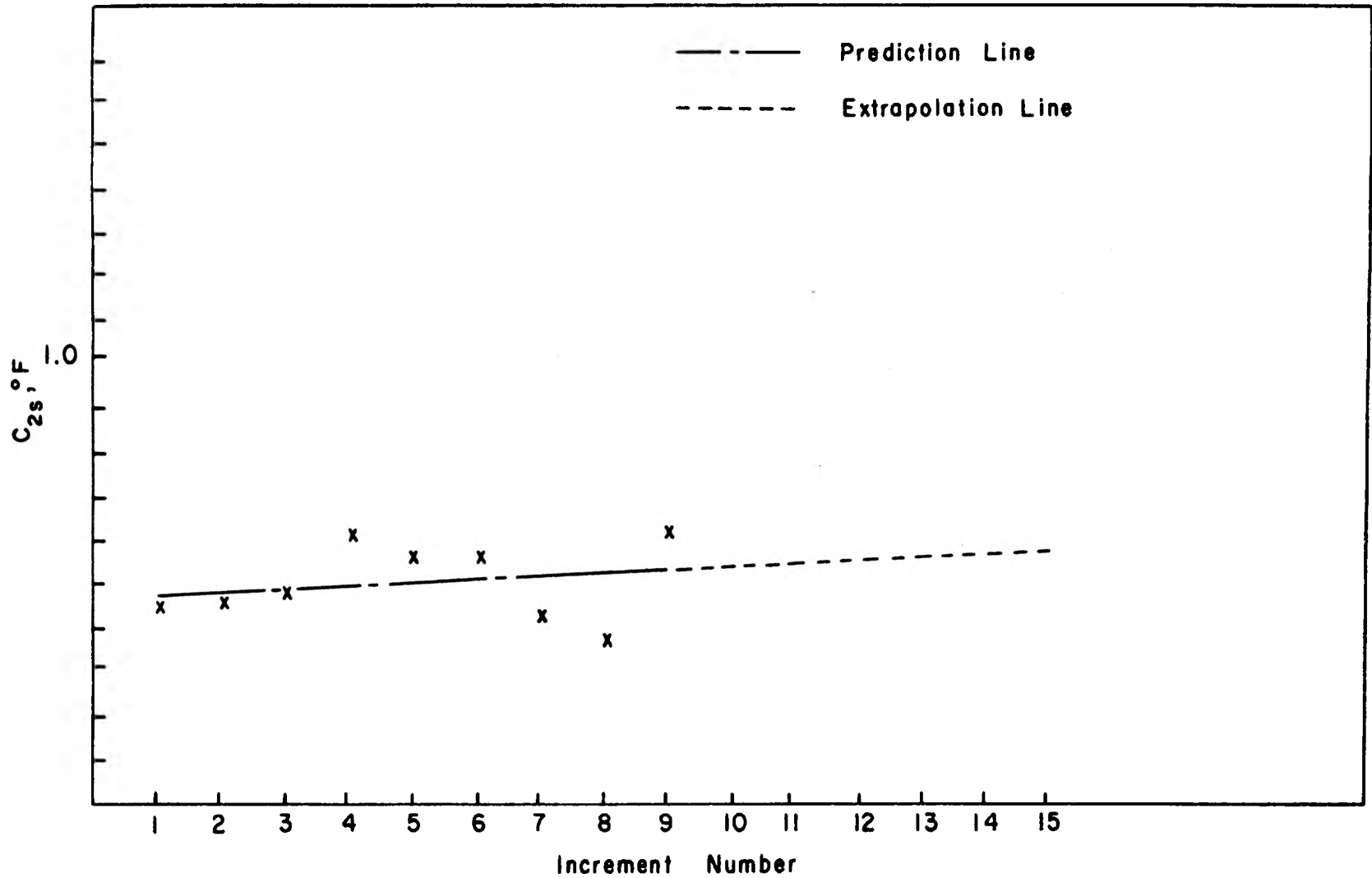
Figure 19. 90-day Regression Data Segment for C_{2s} (Moving Average) with Prediction Line and Extended Extrapolation Line.

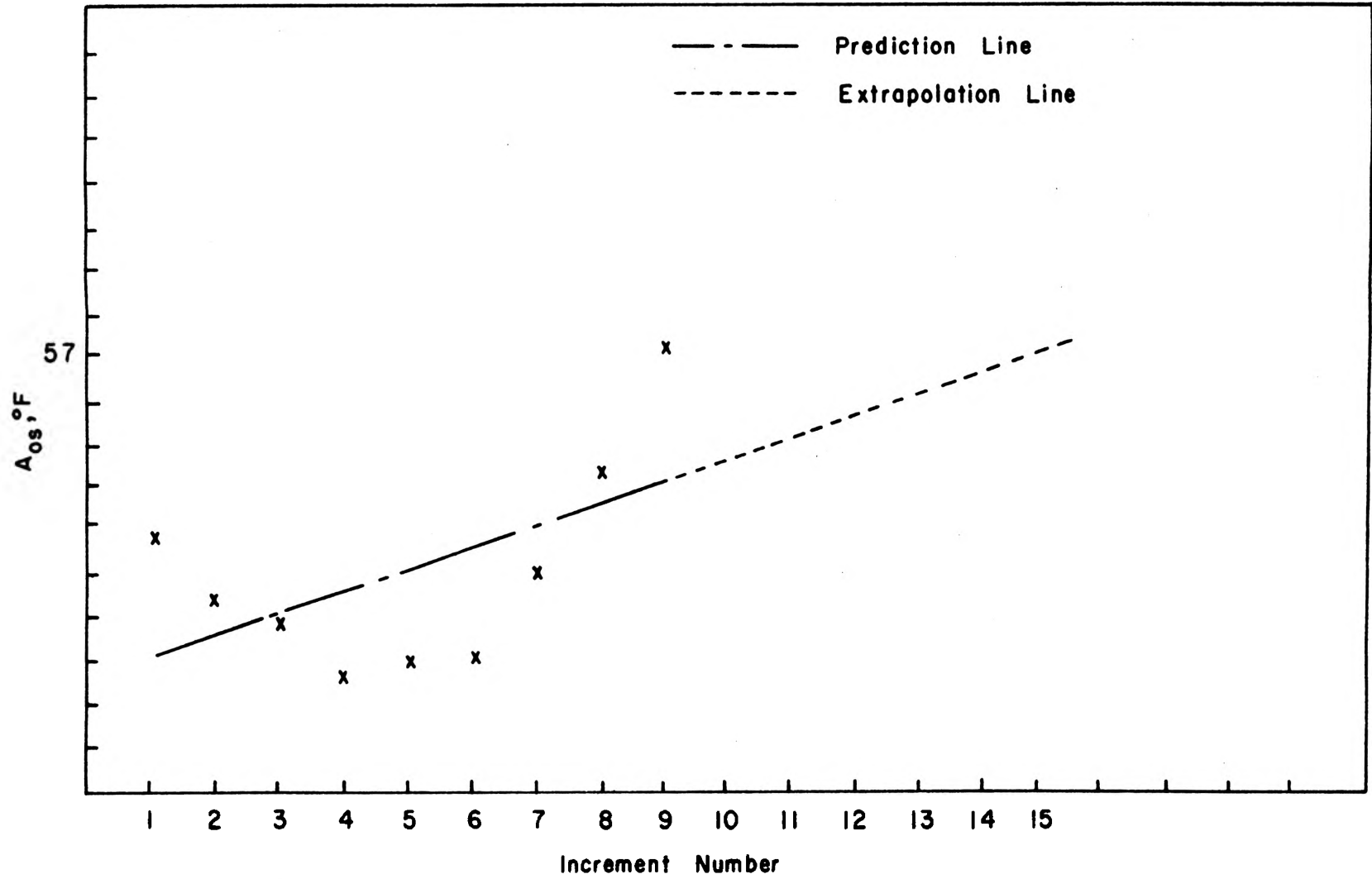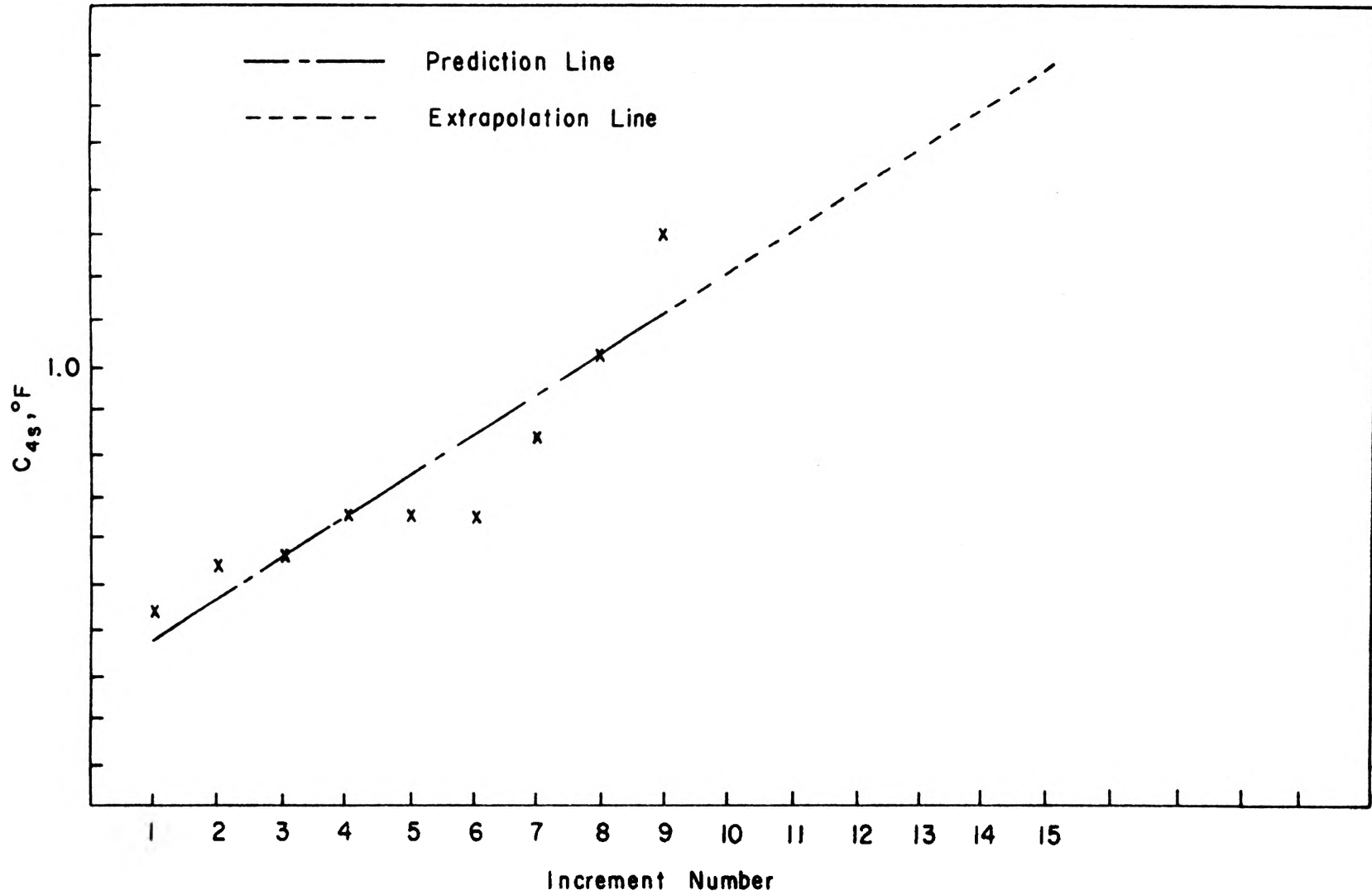Figure 20.   90-day Regression Data Segment for C_{4s} (Moving Average) with Prediction Line and Extended Extrapolation Line.

$$\Delta t_p = \begin{matrix} 10/365 & : & \text{10 day prediction range,} \\ 30/365 & : & \text{30 day prediction range,} \\ 60/365 & : & \text{60 day prediction range.} \end{matrix}$$

Similar predictions were made using (a) A_{op}, C_{1p}, and C_{2p}, and (b) A_{op}, C_{1p}, C_{2p}, and C_{4p}. The use of C_{4p} was prompted by the fact that the spectral content of the daily average data indicated a significant 4 cycle/year peak which was increasing in amplitude over the prediction range. This fact is verified by the increase in C_4 and the corresponding prediction of a further increase by the prediction line shown in Figure 20. The resultant prediction equations are:

$$\text{(a)} \quad X_{p2}(t_i) = X_{p1}(t_i) + C_{2p} \cdot \sin(4\pi t_i + \phi_2), \text{ and}$$

$$\text{(b)} \quad X_{p3}(t_i) = X_{p2}(t_i) + C_{4p} \cdot \sin(8\pi t_i + \phi_4). \tag{36}$$

The results of the temperature forecast are presented graphically in Figures 21, 22, and 23. Each figure shows a plot of the predicted daily average water temperature along with the actual temperature for a prediction range of 60 days. Similar results were obtained for the 10 day and 30 day prediction range. The three figures represent, respectively, temperature predictions using (a) A_{op} and C_{1p}, (b) A_{op}, C_{1p}, and C_{2p}, and (c) A_{op}, C_{1p}, C_{2p}, and C_{4p}.

The values of A_{op}, C_{1p}, C_{2p}, and C_{4p} for the 60-day prediction interval are summarized in Table II on page 64. This table also lists the corresponding values of A_o, C_1, C_2, and C_4 which were calculated from the 365 data points
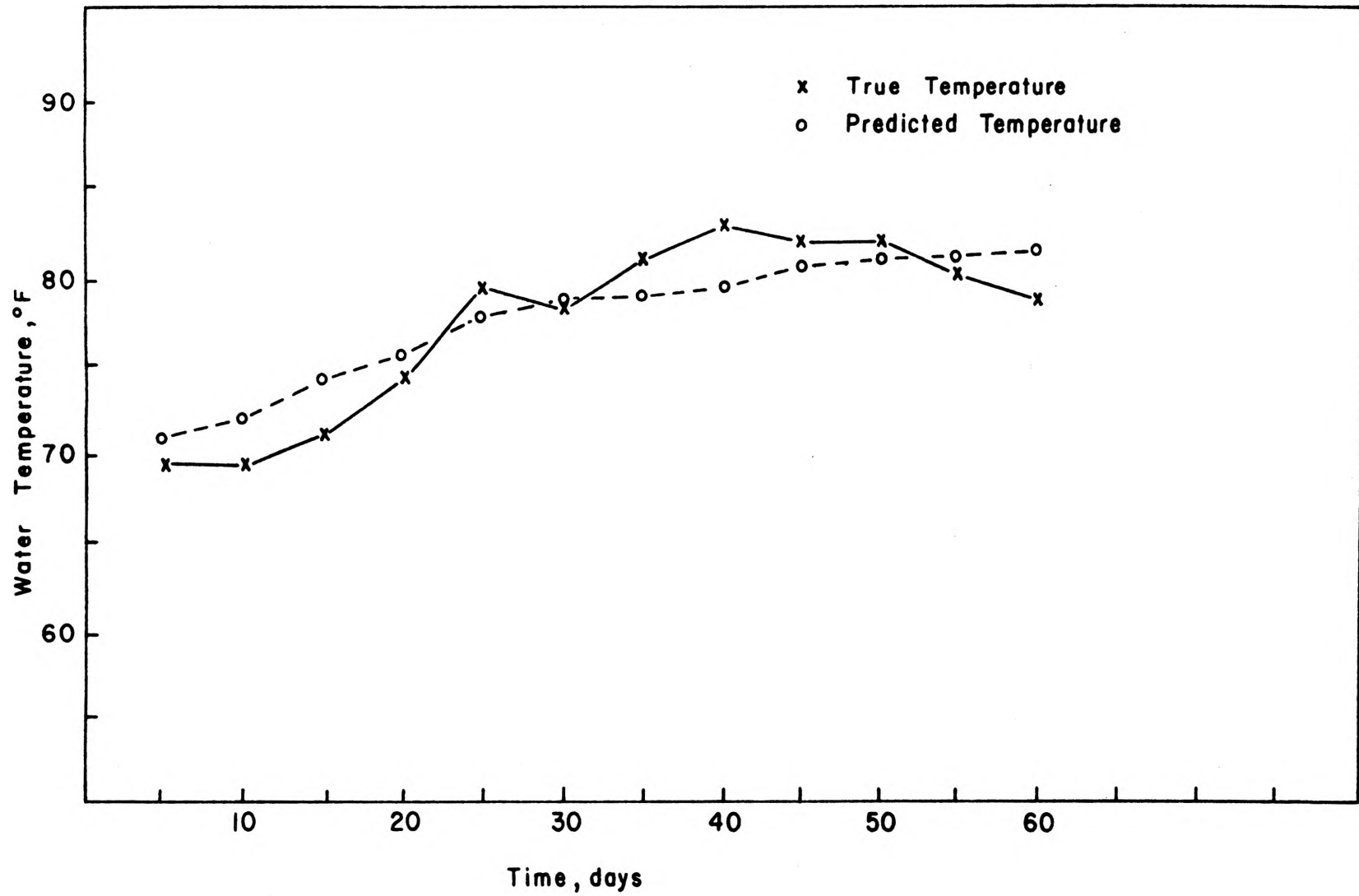
Figure 21. 60-day Water Temperature Predictions Using A_{op} and C_{1p}.
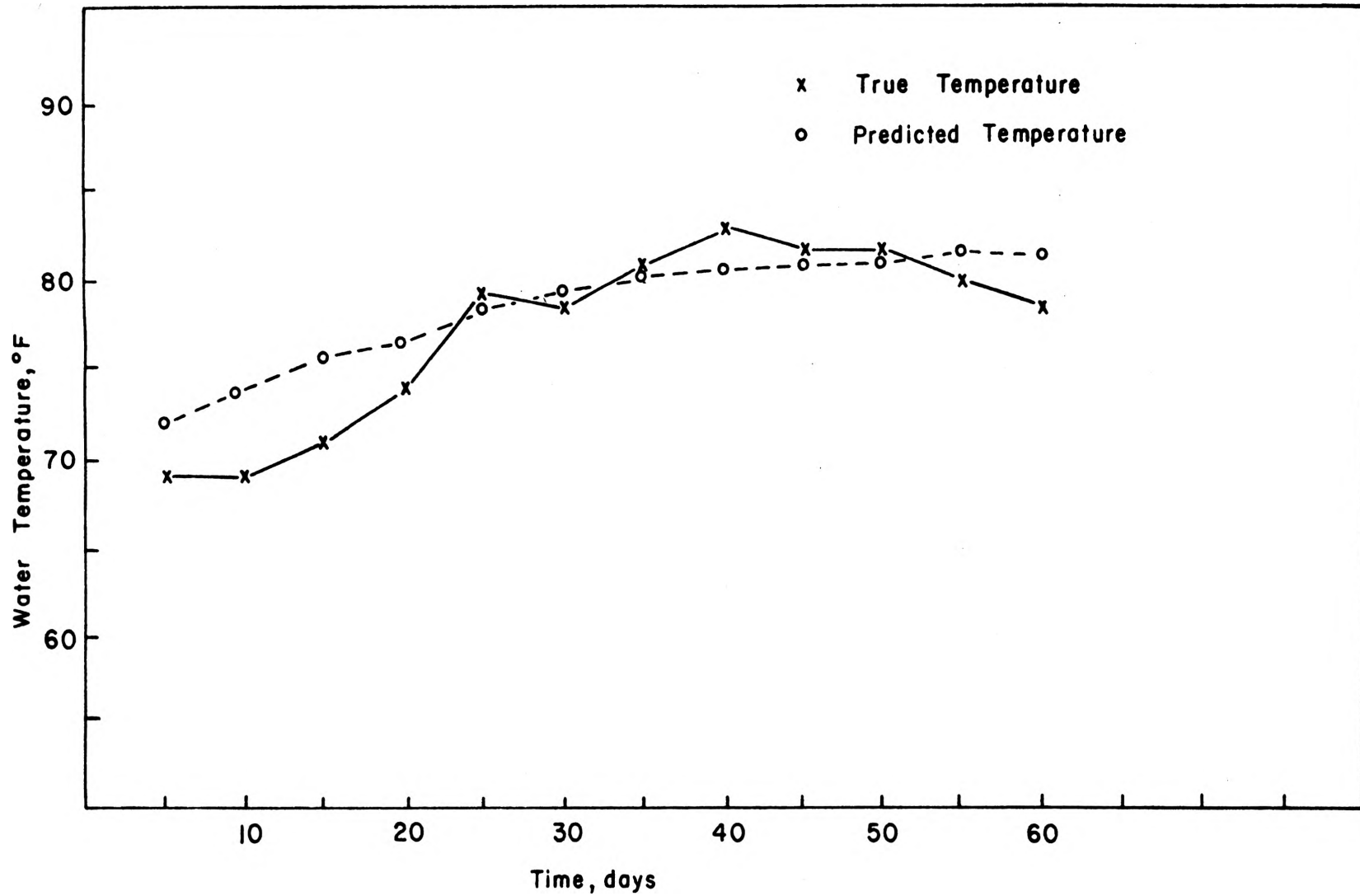
Figure 22. 60-day Water Temperature Predictions Using A_{op}, C_{1p}, and C_{2p}.
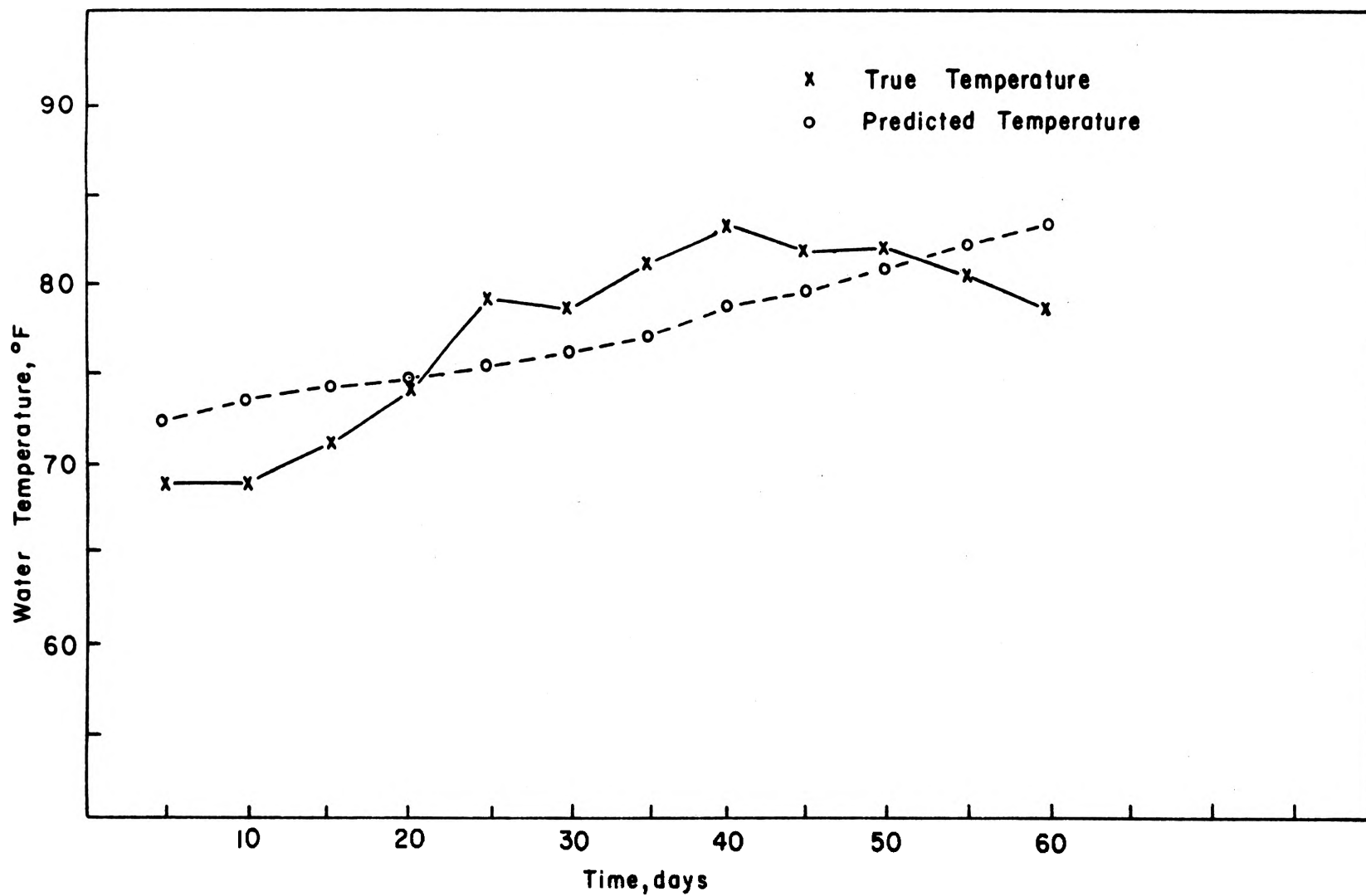
Figure 23. 60-day Water Temperature Predictions Using A_{op}, C_{1p}, C_{2p}, and C_{4p}.

TABLE II

SUMMARY OF CALCULATED TRUE AND PREDICTED
VALUES OF FOURIER COMPONENTS

Component	True Value, °F	Predicted Value, °F	Magnitude of Error, °F
A_o	57.02	56.21	1.81
C_1	12.24	12.26	-0.02
C_2	0.56	0.68	-0.12
C_4	1.65	1.19	0.46

TABLE III

STATISTICS FOR PREDICTION RESIDUALS AND TRUE
RESIDUALS USING (1) A_{op}, C_{1p}, C_{2p}, AND C_{4p},
AND (2) A_o, C_1, C_2, AND C_4

Statistic	Prediction Residuals, $X(t_i) - X_p(t_i)$	True Residuals, $X(t_i) - X_c(t_i)$
$\bar{X}$	0.10	0.18
σ_E	3.24	2.80

corresponding to the 60-day prediction interval plus the preceding 305 data points. Thus, these values represent the true values of A_o, C_1, C_2, and C_4 which were approximated by A_{op}, C_{1p}, C_{2p}, and C_{4p}. The errors in the predictions, which are also summarized in Table II, are thus

$$\epsilon_o = A_o - A_{op},$$

$$\epsilon_1 = C_1 - C_{1p},$$

$$\epsilon_2 = C_2 - C_{2p}, \text{ and}$$

$$\epsilon_4 = C_4 - C_{4p}.$$

The statistics for the residuals $D(t_i) = X(t_i) - X_p(t_i)$, which were obtained by use of predicted values of A_o, C_1, C_2, and C_4, are summarized in Table III. For comparison, Table III also shows a statistical summary of the temperature residuals which were calculated by using the true values of A_o, C_1, C_2, and C_4. In this case the residual set is obtained from the equation

$$D(t_i) = X(t_i) - X_c(t_i) \tag{37}$$

where

$$X_c(t_i) = \overline{X} + C_1 \cdot \sin(2\pi t_i + \phi_1) + C_2 \cdot \sin(4\pi t_i + \phi_2)$$
$$+ C_4 \cdot \sin(8\pi t_i + \phi_4). \tag{38}$$

Examination of the graphs and the table show that the

prediction is very good for the 60-day range which was covered.

E. <u>Analysis of Residuals</u>

One aim of this research was the establishment of some useful conclusions regarding the residual records corresponding to the various regression analyses which were used. If, for example, one is to use the estimation process which was discussed in section C then it must be established that the residuals which remain after the extraction of the harmonic components are normal random variates with zero mean. It would also be of value to know what the expected minimum attainable set of residuals (in the least-squares sense) might be.

In order to obtain some feeling for what the expected minimum attainable set of residuals is, the Minimum Sum of Squares (MINSS) method was developed. This method was developed on the basis of the existence of trends in the data record as discussed in the section on long-term power spectral density calculations. In addition to long-term trends, one might consider the existence of short-term trends as well. Such a trend was represented for purposes of analysis by the linear expression $a - 2at$, $0 \leq t \leq T$, where T is taken as a one-year data segment. Using this trend representation, the MINSS method was formulated by the following algorithm:

(1) Form the detrended time-series

$$X_d(t_i) = X(t_i) - (\Delta a - 2 \cdot \Delta a \cdot t_i)$$

with i = 1, 2, . . ., 365,

Δa = increment in trend slope.

(2) Extract Fourier components 1 through 10 to obtain
the detrended residual set, $D_d(t_i)$.

(3) Form the sum $\sum_{i=1}^{365} D_d(t_i)^2$.

(4) Continue steps 1, 2, and 3 with increments in the
slope of the trend until the value

$$\min \sum_{i=1}^{365} [D_d(t_i)]^2$$

is attained.

The MINSS method was used for all years of record. For
the 1953 record year a value $\min \sum_{i=1}^{365} [D_d(t_i)]^2$ of 1540 $(°F)^2$
was obtained. This corresponds to a deviation of 2.05° F.
Thus, in general, for extraction of 10 Fourier harmonics it
is to be expected that a lower bound on the deviation would
be in the neighborhood of 2° F.

In order to further typify these residuals corresponding
to $\min \sum_{i=1}^{365} [D_d(t_i)]^2$ a histogram was obtained for the
residuals obtained from the 1953 year of record. These same
residuals were tested using the Kolmogorov-Smirnov test and
were found to meet the requirements for normal random
variates with $\sigma = 2.05$ and zero mean. The histogram and the
corresponding cumulative distribution function are shown in
Figure 24.

This same set of residuals was taken to be the normal
random process with mean zero which was assumed in the
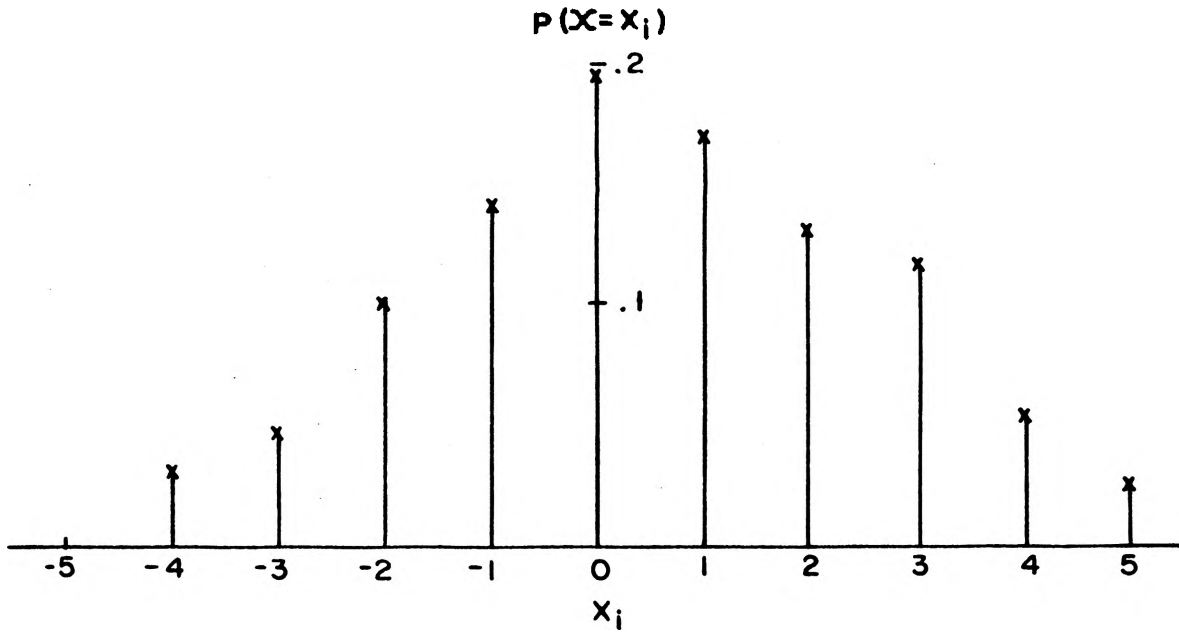
Figure 24 (a).   Histogram for MINSS Residuals-1953 Record.
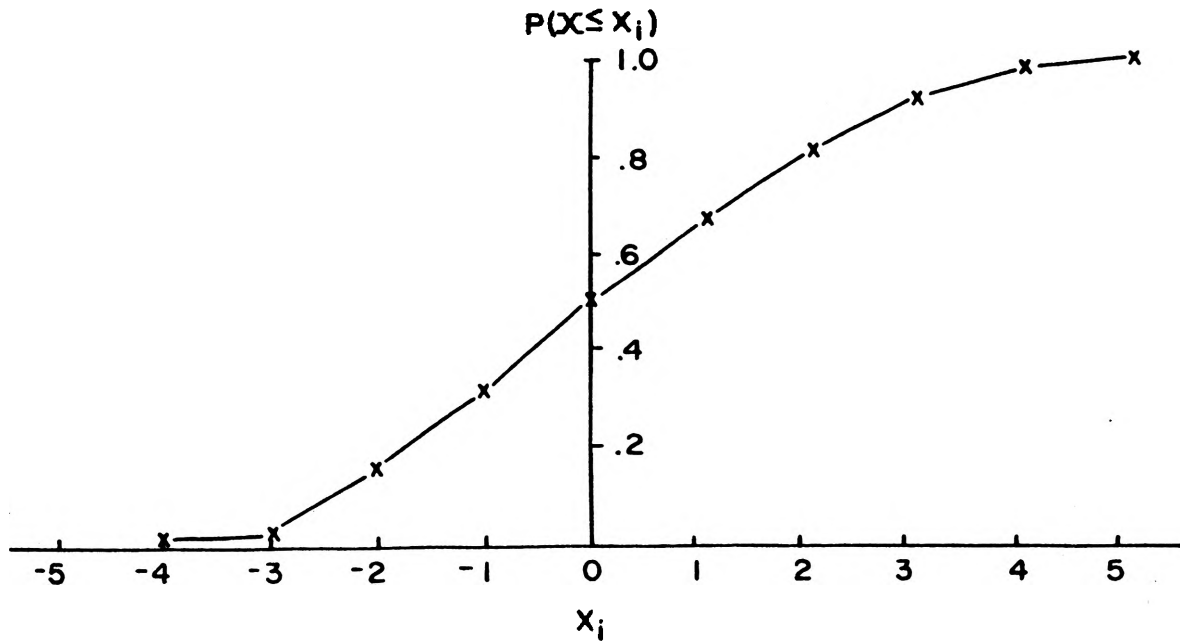
Figure 24 (b).   Cumulative Distribution Function Fit for MINSS
Residuals-1953 Record.

analysis of the estimation process. In this case the constant input U_o was taken as $1°$ F. The processing consisted of taking $\frac{1}{K} \sum_{i=1}^{K} [\min[D_d(t_i)] + U_o] = \hat{U}_o$ for values of K corresponding to 1/5-year, 2/5-year, 3/5-year, 4/5-year, and one-year sample intervals. The values of $\hat{U}_o$ for these sample intervals were $1.075°$ F, $1.003°$ F, $1.010°$ F, $0.973°$ F, and $1.002°$ F respectively. Thus it can be seen that the estimator is very accurate, when the MINSS residuals are used, even for sample records which are considerably less than one year in length.

If MINSS is not used in the predictor analysis, then a verification of the approximate normality of the residuals still needs to be made. This was done for the first year of the 1960-64 data set. The approach here was as follows:

(1) extract fundamental harmonic component

(2) apply Kolmogorov-Smirnov test to residuals

(3) obtain $\frac{1}{K} \sum_{i=1}^{K} D(t_i)$ for K = 10, 20, . . ., 360

(4) extract second harmonic component from the first
     set of residuals and repeat steps (2) and (3).

This process was repeated until the first 10 harmonic components were extracted. The results of the Kolmogorov-Smirnov test are shown in Figure 25 for the residuals with (a) the fundamental extracted and (b) with the first 10 harmonic components extracted.

The graphs of the residual average values, $\frac{1}{K} \sum_{i=1}^{K} D(t_i)$, for the extraction of harmonic components 1 and 2 are shown in Figure 26. It is seen from these graphs that the required
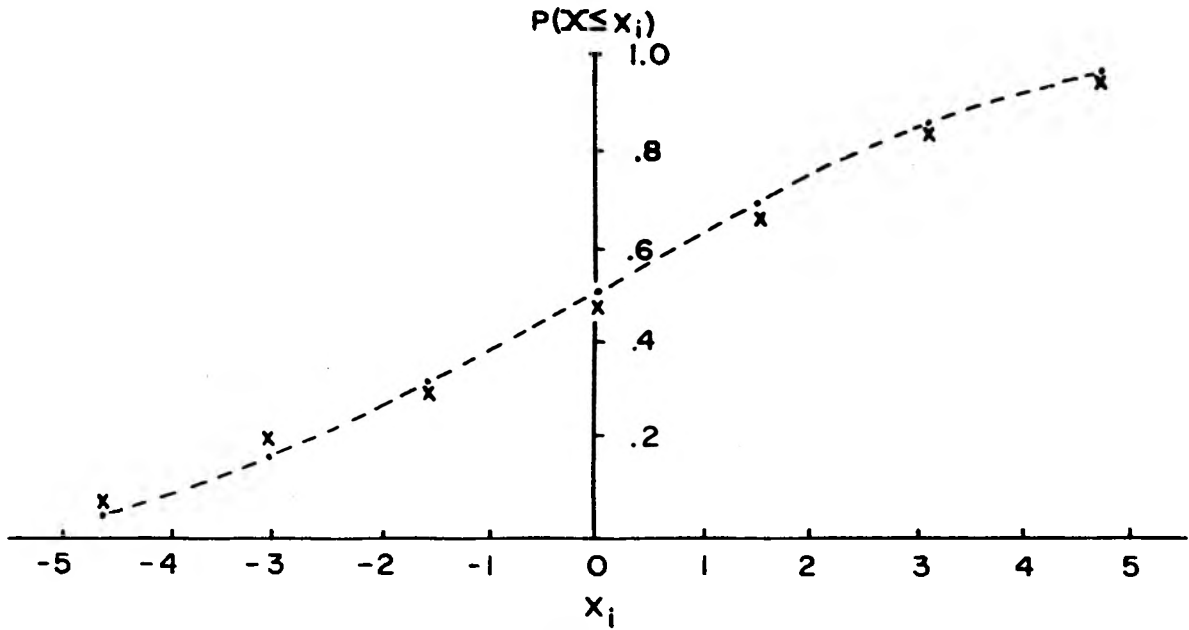
Figure 25 (a). Cumulative Distribution Function Fit for 1960
Record with $\overline{X}$ and Fundamental Extracted.
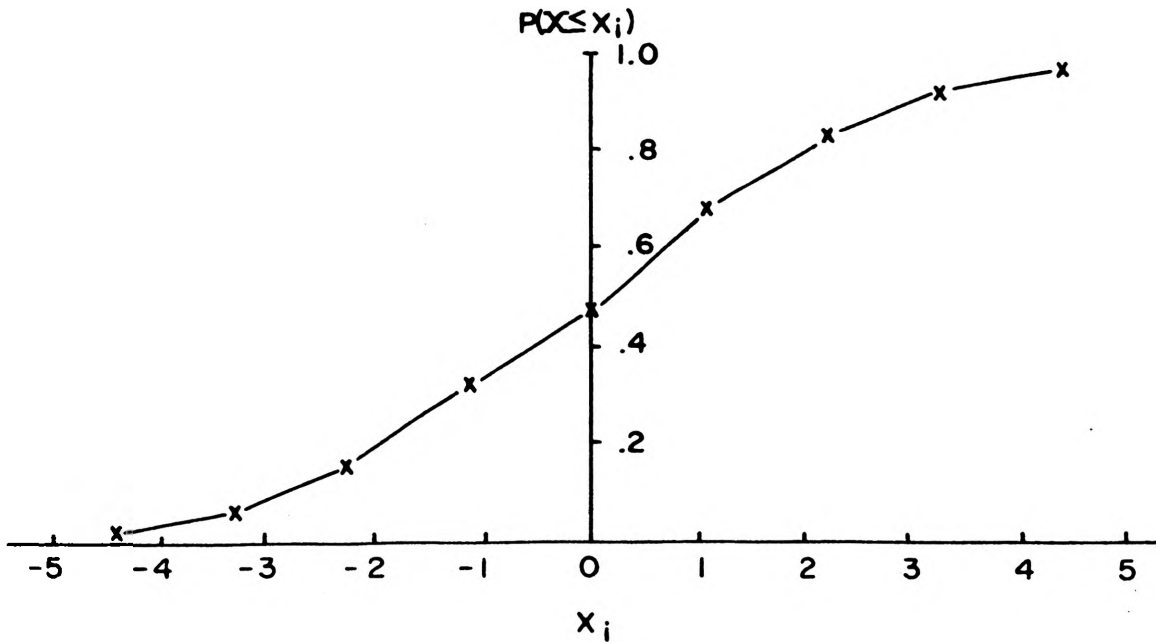
Figure 25 (b). Cumulative Distribution Function Fit for 1960
Record with $\overline{X}$ and First Ten Harmonics Removed.
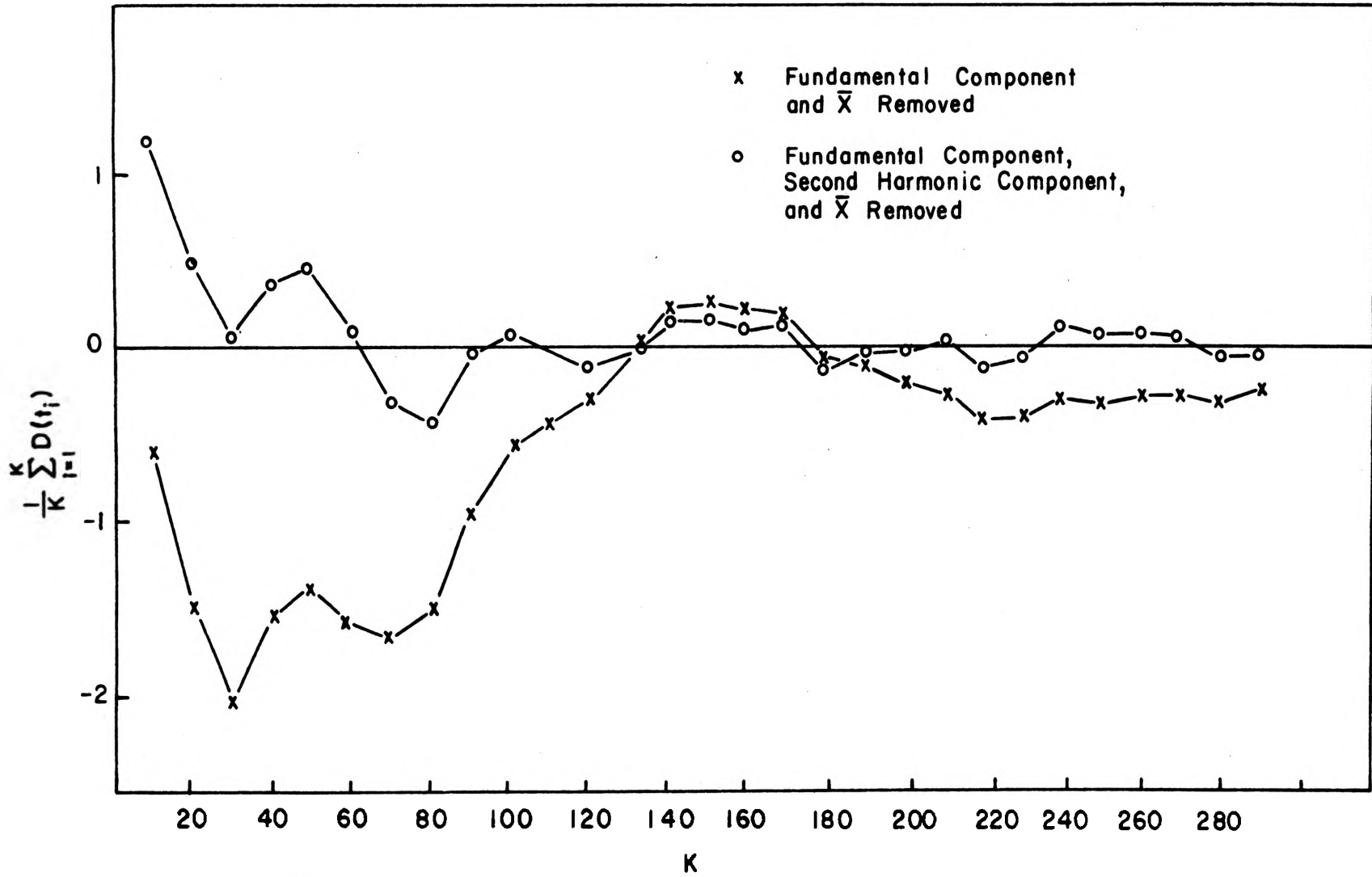
Figure 26. Residual Averages for 1960 Record.

number of days for the average of the residuals to approach
zero is reduced considerably when the second harmonic compon-
ent is extracted.

It is informative to determine the number of daily
samples needed for a given number of extracted harmonics to
reduce the residual average to a value below a fixed bound.
For example, a bound of 0.2° F was used with the result that
290 samples were needed with only the fundamental removed.
When both the first and second harmonics were removed, the
number of samples needed was found to be only 80. A plot of
the number of samples needed to reduce the residual averages
to a value less than or equal to 0.2 versus the number of
harmonics extracted is shown in Figure 27. It is seen from
this plot that extraction of Fourier components beyond the
second harmonic will have little effect in reducing the
number of samples needed to bring the average value of the
residuals close to zero. Thus it may be reasonable to
expect, at least from the estimation point of view, that
extraction of only the fundamental and the second harmonic
components will give good results when a one-year data
segment is used.

F. Suggested Form for Regression Model

As in any model-building process one should never be
completely satisfied with results which, in the model-
builders opinion, can be improved upon. Thus, based upon
both the power spectral density analysis of Chapter III and
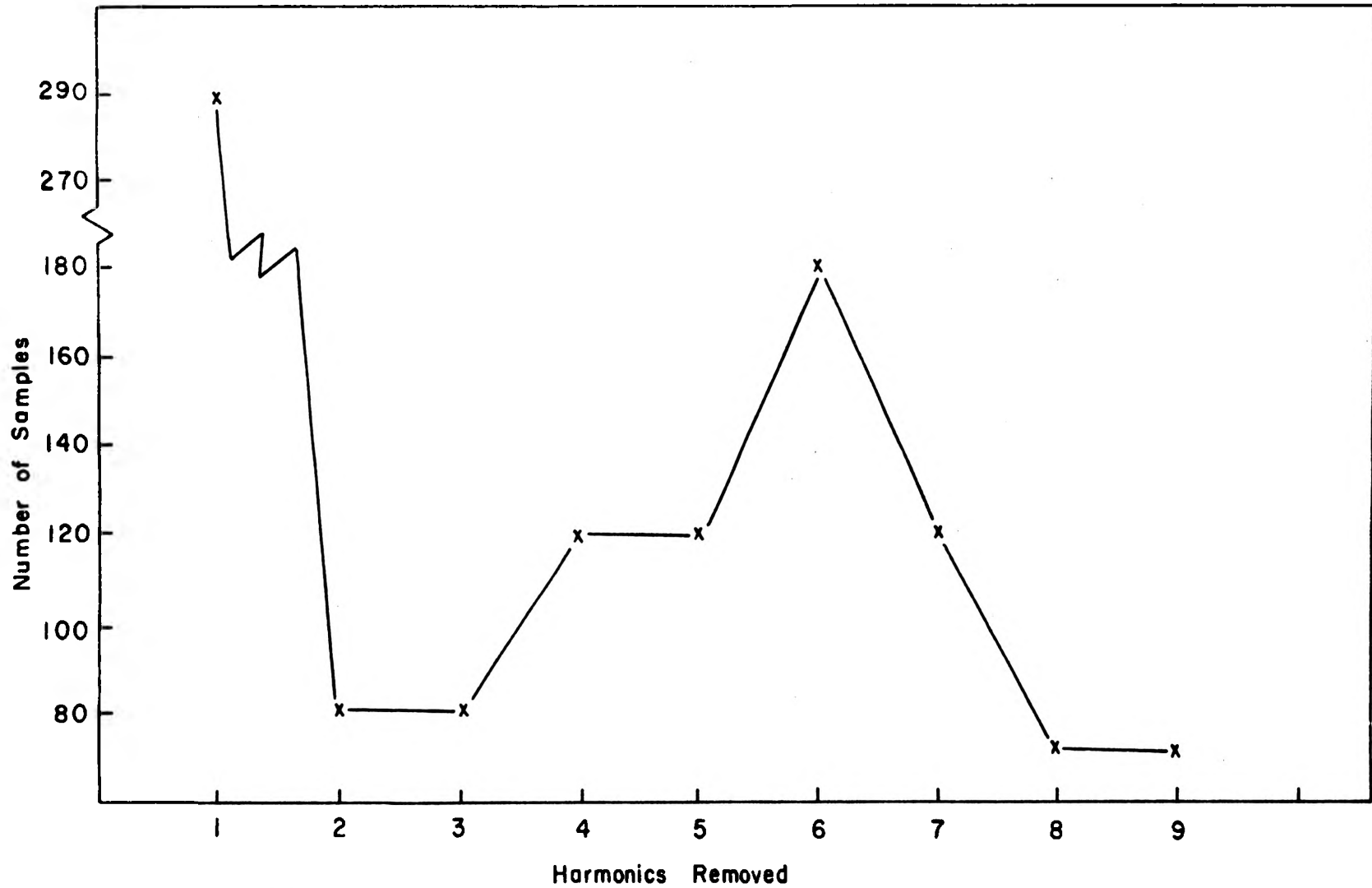
Figure 27.   Samples Needed to Satisfy $\frac{1}{K} \sum_{i=1}^{K} D(t_i) \leq 0.2$ for 1960 Record.

the regression analyses presented in this chapter, the
following final model for river water temperatures is
proposed:

$$X(t) = A_o(t) + \sum_{k=1}^{n} C_k(t) \cdot \sin(2\pi kt + \phi_k)$$

$$+ \{C_f(t) \cdot \sin(2\pi ft + \phi) : n < f \leq 10\} + \eta(t) \qquad (39)$$

where the model components are

(1) $A_o(t)$: slowly varying component,

(2) $\sum_{k=1}^{n} C_k(t) \cdot \sin(2\pi kt + \phi_k)$: periodic components
which are harmonically related to the one cycle/year
component,

(3) $\{C_f(t) \cdot \sin(2\pi ft + \phi) : n < f \leq 10\}$: frequency
components which are not harmonically related to
the one cycle/year component, and

(4) $\eta(t)$: normal random noise.

Actually, components (1) and (2) together form the general
shape of the temperature curve which, as previously mentioned,
closely resembles a sinusoid plus a steady-state component.
However, it was observed that, characteristically, the
temperature recordings remained near 32° F for a time period
of about three months during the winter. Thus, the time-
domain representation of the water temperature is more
accurately described by a steady-state component with a
clipped sinusoid. This means that, at most, three (n = 3)
Fourier terms would be needed in component part (2) to

adequately describe the general shape of the temperature curve.

The spectral peaks which occurred at frequencies beyond three cycles/year are not, by the nature of their occurrence, harmonically related to the clipped sinusoid. They were picked up, as any spectral components would be, by both the power spectral density analysis and the Fourier regression analysis. However, the previously noted lack of persistency of these peaks show that they can be thought of as wavelets which appear at various seasons of the year (in particular in the spring) and then decay. Since these wavelets are temporary in nature, Fourier analysis would not give a true representation of their strength within the time-period for which they occur.

That this is true can be shown by consideration of a sinusoidal wavelet having a period of 1/5 year (5 cycles/year). The wavelet, however, is assumed to exist for only one complete cycle for each year of record. This is illustrated by the waveform shown in Figure 28 (a). The corresponding amplitude spectrum for this wavelet is shown in Figure 28 (b). Thus, the Fourier analysis would result in a 5 cycle/year sinusoidal component with amplitude $1/5°$ F rather than the peak amplitude of $1°$ F which the wavelet actually possesses. The remaining cyclic components which are represented in the amplitude spectral plot would, of course, sum with this 5 cycle/year component to yield the waveform of Figure 28 (a). Thus, if one is willing to accept the less-accurate

$$e(t) = \begin{cases} \sin\frac{2\pi}{5}t & ; \; 0 \le t \le \frac{1}{5} \\ 0 & ; \; \frac{1}{5} \le t \le 1 \end{cases}$$

e(t) Periodic
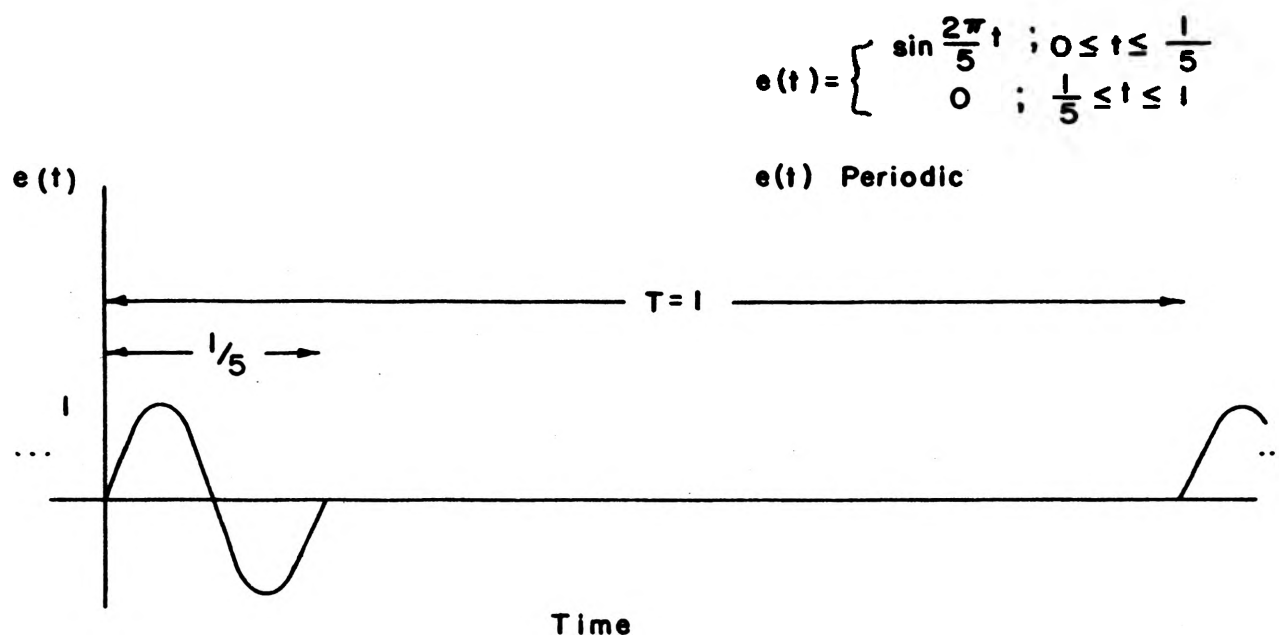
Figure 28 (a).   5-Cycle Wavelet Which Persists for 1/5
Period.
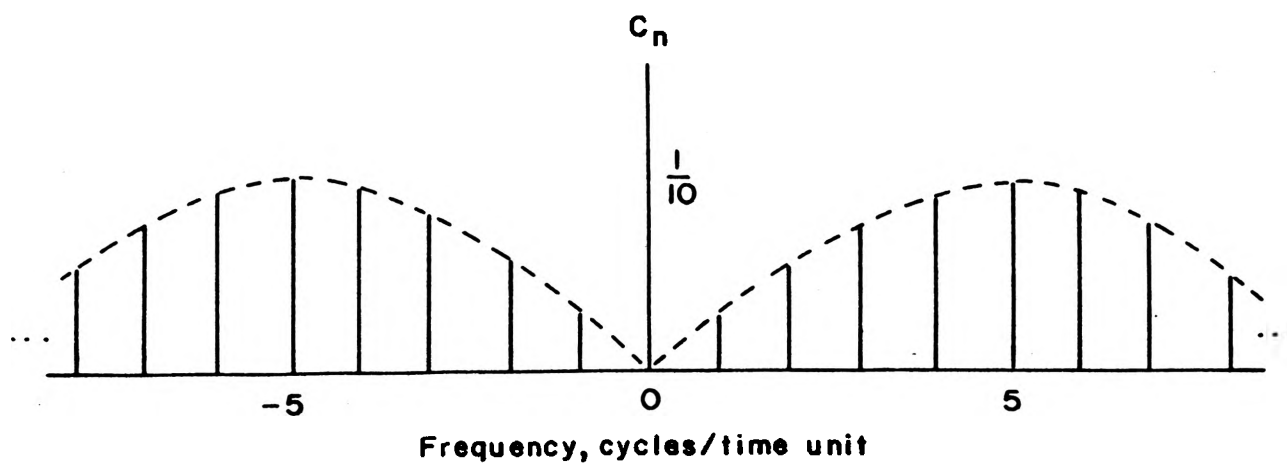
Figure 28 (b).   Amplitude Spectrum for (a).

temperature prediction, then, based upon the results presented in this chapter, the prediction equation

$$X(t_i) = A_{op} + \sum_{k=1}^{2} C_{kp} \cdot \sin(2\pi k t_i + \phi_k) \qquad (40)$$

should consistently yield predicted temperatures within a standard deviation of about 3° F.

If the wavelet effects represented by $C_f(t) \cdot \sin(2\pi ft + \phi)$ are deemed critical, then the prediction method for $C_f(t)$ should be based on a combination of the use of power spectral density methods and what will be called sample-interval scanning. This latter technique would consist of scanning across the one-year sample interval using sub-divided sample intervals which would correspond to the particular frequency (wavelet) being sought. For example, a scan across the time interval of $0 \le t \le 1$ (year) in Figure 28 (a) would only yield nonzero values for the 5 cycle/year cyclic component when the scan is in the interval $0 \le t \le 2/5$.

As mentioned in the introductory remarks, the prediction of the water temperature should prove valuable to both power companies and to water quality control groups. In discussing this particular aspect of this problem with Dr. Derald Morgan, Electrical Engineering Department, University of Missouri-Rolla, it was found that most of the large fossil-fuel plants which are presently being planned are expected to have a constant output power level. Thus,

it is to be expected that the representation of the thermal input to the cooling medium by the constant, U_o, is reasonable.

This means that the predictive equation would take this input into account by addition. Thus the prediction equation for river temperature becomes:

$$X(t_i) = U_o + A_{op} + \sum_{k=1}^{2} C_{kp} \cdot \sin(2\pi kt_i + \phi_k). \qquad (41)$$

This model should provide an effective means whereby water quality control standards can be assured.

V. CONCLUSIONS

The results presented in this dissertation demonstrate the applicability of power spectral density techniques and linear regression analysis, especially Fourier series regression analysis, to the mathematical modeling of river water temperature.

The existence of long-term fluctuations was verified in Chapter III by power spectral density calculations for 5-year and 3-year record lengths. These calculations, which are plotted in Figures 2 and 3, show that to attempt an accurate prediction of future values of river water temperature on the basis of any single segment of data would be impossible. This includes one-year segments which correspond to the large yearly seasonal fluctuation of river water temperature.

The power spectral density calculations for both the long-term records and the one-year records were made after removal of the one cycle/year temperature component. The power spectral density calculations for the one-year records revealed the existence of fluctuations in the amplitude of spectral peaks which existed in the frequency range of 0 to 10 cycles/year. The fluctuation in the amplitude of these spectral peaks was further demonstrated by Fourier series calculation of the amplitude of the various components which were harmonically related to the one cycle/year fluctuation. These results led to the conclusion that a representation of these fluctuations would be best represented by the time-

domain function

$$C_k(t) \cdot \sin(2\pi kt + \phi_k)$$

where $C_k(t)$ is the time-varying fluctuation in the amplitude of the kth harmonic component and ϕ_k is the initial phase.

Consideration has also been given to the application of communication theory techniques to the estimation of man-made thermal inputs to rivers. The techniques are shown to be applicable in Chapter IV, but a more useful result is that of a mathematical model which allows future values of water temperature to be predicted.

The previously discussed amplitude fluctuations, $C_k(t)$, led to an approximating equation to river water temperature having the form

$$X(t) \cong A_0(t) + \sum_{k=1}^{n} C_k(t) \cdot \sin(2\pi kt + \phi_k)$$

where $A_0(t)$ is the representation of the slowly varying yearly-average of water temperature. This model allows prediction of future values of river water temperature based on predicted values of A_0 and C_k, $k = 1, 2, \ldots, n$.

A test of the predictive capability of the model was made using predicted values of A_0, C_1, C_2, and C_4. These predicted values are, symbolically, A_{op}, C_{1p}, C_{2p}, and C_{4p}. The prediction equation used for the time-series of daily average water temperature was then

$$X_p(t_i) = A_{op} + \sum_{\substack{k=1 \\ k \neq 3}}^{4} C_{kp} \cdot \sin(2\pi kt + \phi_k).$$

The reason for using only C_{2p} and C_{4p}, in addition to A_{op} and C_{1p}, was the fact that they were the only significant power spectral density components, other than the one cycle/year component, which were detected for the particular data segment used in the analysis. The results for a 60-day prediction of A_o, C_1, C_2, and C_4, as summarized in Table II, show that the prediction errors are

$$\epsilon_o = 1.81° \text{ F for } A_o,$$

$$\epsilon_1 = -0.02° \text{ F for } C_1,$$

$$\epsilon_2 = -0.12° \text{ F for } C_2, \text{ and}$$

$$\epsilon_4 = 0.46° \text{ F for } C_4.$$

Further consideration of all phases of the study led to the conclusion that the mathematical model should be divided into four component parts as expressed by the equation

$$X(t) = A_o(t) + \sum_{k=1}^{n} C_k(t) \cdot \sin(2\pi kt + \phi_k)$$

$$+ \{C_f(t) \cdot \sin(2\pi ft + \phi) : n < f \leq 10\} + \eta(t)$$

These components are:

    (1) $A_o(t)$: slowly varying component,

    (2) $\sum_{k=1}^{n} C_k(t) \cdot \sin(2\pi kt + \phi_k)$: periodic components which

are harmonically related to the one cycle/year
component,

(3) $\{C_f(t) \cdot \sin(2\pi ft + \phi) : n < f \leq 10\}$: frequency
components which are not harmonically related to
the one cycle/year fluctuation,

(4) $\eta(t)$: normal random noise.

This model allows the capability of (1) rough prediction
based on the model components one and two and (2) finer
prediction based on model components one, two, and three.
The addition of model component three gives the capability
of predicting the short-term seasonal fluctuations which may
last for time periods of less than one full year. The
assumption that component four is a normal random variable
with zero mean is a valid hypothesis on the basis of the
Kolmogorov-Smirnov tests applied to the residual data.

It is felt that model component three of the water
temperature model would furnish a fruitful research subject
for future study. It was observed that, in addition to the
fluctuations in the amplitude components, $C_k(t)$ and $C_f(t)$,
the frequency changed for some of the power spectral density
peaks. Thus a three-dimensional plot similar to that shown
in Figure 7, only with increments less than 30 days, would
furnish useful information about these frequency variations.
It might be well to consider the inclusion of these frequency
changes in the modeling process.

Another possible area for further investigation is that
of applying power spectral density techniques to the

statistical analysis of non-stationary random processes. This would, in effect, involve the extraction of polynomial fits to samples which appear to be normal random variates but which actually contain long-term trends. The presence of long-term trends in the data will, when spectrally analyzed, appear somewhat like the spectral plot shown in Figure 2. One could then fit the data to various polynomials, extract the polynomials, and then assume that the best fit to the trend is that polynomial which yields the smallest low-frequency spectral output.

Further work also needs to be done toward implementing the proposed prediction models. This would involve the collection of more data, the regression fits to the data, and a corresponding prediction of future water temperatures based on the proposed model. A check of the accuracy of the model could then be made by the closeness of the predicted temperatures to the true temperature.

BIBLIOGRAPHY

1. A Panel Report. "Water Quality Control," Proceedings of the American Society of Civil Engineers, Journal of the Power Division, Vol. 96, No. P02, February 1970, pp. 221-229.

2. Friedlander, Gordon D., "Power, Pollution, and the Imperiled Environment--Part I," IEEE Spectrum, Vol. 7, No. 11, November 1970, pp. 40-50.

3. Friedlander, Gordon D., "Power, Pollution, and the Imperiled Environment--Part II," IEEE Spectrum, Vol. 7, No. 12, December 1970, pp. 65-75.

4. Morgan, Paul V. and Henry C. Bramer, "Thermal Pollution as a Factor in Power Plant Site Selection," Proceedings of the American Power Conference, Vol. 31, 1969, pp. 724-732.

5. Leung, Paul and R. E. Moore, "Thermal Cycle Arrangements for Power Plants Employing Dry Cooling Towers," Journal of Engineering for Power, ASME, Vol. 93, Series A, No. 2, April 1971, pp. 257-264.

6. Hartwig, L. E. and J. J. Rechner, "Air and Thermal Pollution in the Power Industry: Causes, Control Equipment, Economics and the Power Industry's Approach," A report submitted to Thomas P. Hertel, Instructor of Electrical Engineering, University of Missouri-Rolla, Spring, 1970.

7. McAllister, R. J., C. N. Lawrence and B. Bradfield, "Control of Thermal Effects at Beaver Valley Station," Proceedings of American Society of Civil Engineering, Journal of the Power Division, Vol. 96, No. P03, June 1970, pp. 287-298.

8. Nobuyuki, T., R. L. Wiegel, and G. F. Tornberg, "Horizontal Surface Discharge of Warm Water Jets," Proceedings of the American Society of Civil Engineers, Journal of the Power Division, Vol. 95, No. P02, October 1969, pp. 253-275.

9. Jaske, R. T., "A Need for Advance Planning of Thermal Discharges Before Site Acquisition," Proceedings of the American Power Conference, Vol. 31, 1969, pp. 733-742.

10. Brown, George W., "Predicting Temperatures in Small Streams," Water Resources Research, Vol. 5, No. 1, February 1969, pp. 68-75.

11. Morse, William L., "Stream Temperature Prediction Model," Water Resources Research, Vol. 6, No. 1, February 1970, pp. 290-302.

12. Chen, Cheng-lung, "Fate of Thermally Polluted Surface Water in Rivers," Proceedings of the American Society of Civil Engineers, Journal of the Sanitary Engineering Division, Vol. 97, No. SA3, June 1971, pp. 311-331.

13. Blackman, R. B. and J. W. Tukey, The Measurement of Power Spectra from the Point of View of Communications Engineering. New York: Dover, 1958.

14. Tukey, J. W., "Discussion, Emphasizing the Connection Between Analysis of Variance and Spectrum Analysis," Technometrics, 3(2), 1961, pp. 191-219.

15. Jenkins, G. M., "General Considerations in the Analysis of Spectra," Technometrics, 3(2), 1961, pp. 133-166.

16. Parzen, Emanuel, Time Series Analysis Papers. San Francisco: Holden-Day, 1967.

17. Jenkins, Gwilym M. and Donald G. Watts, Spectral Analysis and Its Applications. San Francisco: Holden-Day, 1968.

18. Box, George E. P. and Gwilym M. Jenkins, Time Series Analysis, Forecasting and Control. San Francisco: Holden-Day, 1970.

19. Rodriquez-Iturbi, I., "The Application of Cross Spectral Analysis to Hydrologic Time Series," Colorado State University Hydrology Paper 24, Fort Collins, Colorado, 1967.

20. Rodriquez-Iturbe, I. and Carl F. Nordin, "Some Applications of Cross Spectral Analysis in Hydrology: Rainfall and Runoff," Water Resources Research, Vol. 5, No. 3, June 1969, pp. 608-621.

21. Roesner, L. A. and V. Yevjevich, "Mathematical Models for Time Series of Monthly Precipitation and Monthly Runoff," Colorado State University Hydrology Paper 15, Fort Collins, Colorado, 1966.

22. Chapman, S. and J. Bartels, Geomagnetism Volume II. Oxford University Press, 1940, second edition, 1951.

23. Kothandaraman, Veerasamy, "Analysis of Water Temperature Variations in Large River," Proceedings of the American Society of Civil Engineering, Journal of the Sanitary Engineering Division, No. SA1, February 1971, pp. 19-31.

24. Lee, Y. W., _Statistical Theory of Communication_. New York: John Wiley and Sons, 1960.

25. Hancock, John C., _An Introduction to the Principles of Communication Theory_. New York: McGraw-Hill Book Co., Inc., 1961.

26. Selin, I., _Detection Theory_. Princeton: Princeton University Press, 1965.

27. Van Trees, H. L., _Detection, Estimation and Modulation Theory, Part I_. New York: John Wiley and Sons, 1968.

28. Helstrom, Carl W., _Statistical Theory of Signal Detection_. New York: Pergamon Press, 2nd edition, 1968.

29. Bendat, J. S. and A. G. Piersol, _Measurement and Analysis of Random Data_. New York: John Wiley and Sons, 1966.

30. Robinson, E. A., _Multichannel Time Series Analysis with Digital Computer Programs_. San Francisco: Holden-Day, 1967.

31. Rice, John R., _The Approximation of Functions, Vol. 1, Linear Theory_. Reading: Addison-Wesley, 1964.

32. Long, L. L., B. E. Gillett, and J. C. Maxwell, "Detection of Power Plant Thermal Pollution in Rivers by Communications Systems Techniques," Presented at the 40th National Meeting, Operations Research Society of America, Anaheim, California, October 27-29, 1971.

33. Maxwell, J. C., L. L. Long, and E. J. Garrison, "Power Spectral Analysis of Water Temperature Fluctuations," _Joint Conference on Sensing of Environmental Pollutants_, Palo Alto, California, November 8-10, 1971, AIAA Paper No. 71-1126.

34. Gillett, B. E., L. L. Long, and J. C. Maxwell, "Statistical Analysis of Water Temperature Residuals," To be presented at the 41st National Meeting, Operations Research Society of America, New Orleans, Louisiana, April 26-28, 1972.

APPENDIX A

MATHEMATICAL FUNDAMENTALS

A. Approximation of Real Functions

The primary goal of this research has been the develop-
ment of a mathematical model which can be considered to be
the best approximation of the observed fluctuations in river
water temperature. The true temperature function, $X(t)$,
which represents these temperature fluctuations is, by its
very nature, a bounded and continuous real function. Hence,
the problem of building a suitable model for $X(t)$ involves
finding an approximating function, $H(\Psi,t)$, where Ψ represents
a fixed set of parameters. The two major criteria in this
model-building process are (1) the type of approximating
function used and (2) the goodness of fit to the function
$X(t)$. In the discussion which follows the more general
functional notation $f(t)$ will be used as the function to be
approximated.

One widely used measure of the goodness of fit of the
approximating function is that of a distance function
$\rho[f(t),H(\Psi,t)]$ which is used to determine the distance of
$H(\Psi,t)$ from $f(t)$. The function ρ which is considered in
this study is a norm element defined on a function space, V,
and hence has the following properties:

1. $||\rho|| \geq 0$, $||\rho|| = 0$ iff $\rho = 0$

2. $||c\rho|| = |c| \cdot ||\rho||$, for all $c \ \epsilon$ Reals, and

3. $||\rho + \gamma|| \leq ||\rho|| + ||\gamma||$, for all $(\rho,\gamma)\epsilon V$.

The best approximation of a real-valued continuous function f(t) is defined to be a solution to the following problem:

Given that f(t) is a real-valued continuous function, let $H(\Psi,t)$ be a real-valued approximating function which depends continuously on t and on the parameter set Ψ. Given the distance function ρ, find the parameter set Ψ^* such that

$$\rho[f(t),H(\Psi^*,t)] \leq \rho[f(t),H(\Psi,t)]$$

for all Ψ.

For the purpose of this analysis, f(t) is considered to be a member of the class of norms called L_p-norms. The L_p-norm of the function f(t), as defined on the real interval [0,1], is defined by the relation

$$L_p = [\int_0^1 |f(t)|^p \, dt]^{1/p}, \quad p \geq 0. \tag{A-1}$$

The best L_p approximation to f(t) is found by minimization of the L_p distance function

$$[\int_0^1 |f(t) - H(\Psi,t)|^p \, dt]^{1/p}.$$

In order to be useful, the general form of the approximating function $H(\Psi,t)$ must be replaced by a specific function type which, in this analysis, is a linear approximating function. The linear approximating function is given by

$$H_L(\Psi, t) = \sum_{i=1}^{n} a_i \, \alpha_i(t) \qquad \text{(A-2)}$$

where a_i, $i = 1, 2, \ldots, n$, are real constants and $\alpha_i(t)$, $i = 1, 2, \ldots, n$, are real-valued functions of the real variable t. The $\alpha_i(t)$ functions are assumed to be linearly independent.

The most widely used norm for linear approximating functions is the L_2-norm which results in the least-squares approximation of f(t) given by

$$L_2(f - H_L) = [\int_0^1 [f(t) - H_L(\Psi, t)]^2 dt]^{1/2}. \qquad \text{(A-3)}$$

This norm has the advantage that, with the use of the linear approximating function, it is possible to obtain explicit expressions for the elements of the set Ψ which constitute the coefficients of H_L. Also, it can be shown that unique best-approximations to f(t) exist.

With the use of the linear approximating function $H_L(\Psi, t)$ and the L_2-norm, the criterion used to measure the goodness of fit to f(t) is the minimization of $L_2(f - H_L)$. That is, obtain the set of coefficients, Ψ, which minimizes the distance between f(t) and $H_L(\Psi, t)$ in the least-squares sense. The minimization process is simplified by minimizing $[L_2(f - H_L)]^2$ rather than $L_2(f - H_L)$.

Thus, the minimization process involves taking the partial derivative

$$\frac{\partial}{\partial a_i} \int_0^1 [f(t) - H_L(\Psi,t)]^2 \, dt = \int_0^1 \{\frac{\partial}{\partial a_i}[f(t) - H_L(\Psi,t)]^2\} dt$$

$$= -2 \int_0^1 \{[f(t) - H_L(\Psi,t)] \cdot \frac{\partial}{\partial a_i}[H_L(\Psi,t)]\} dt.$$

Setting this partial derivative equal to zero will then yield the desired parameter set Ψ^*.

A widely used application of this technique is that of least-squares polynomial regression analysis. It is also used in the development of Fourier series approximations to real periodic functions.

B. Fourier Series

Since river water temperature exhibits a predominant yearly seasonal function which is almost periodic, it is worthwhile to consider the study of approximations to periodic functions. The accepted approach for this type of approximation is through the use of Fourier series. It is useful to first state the following definitions.

Definition 7. A real-valued time-domain function $g(t)$ is said to be periodic with period T if for all $t \geq 0$,

$$g(t) = g(t + kT), \quad k = 0, \pm 1, \pm 2, \ldots$$

Definition 8. A function $G(t)$ is said to be a real harmonic with radian frequency ω and amplitude A, where ω and A are positive constants, if it is either of the form

$$G(t) = A \cdot \cos(\omega t)$$

or

$$G(t) = A \cdot \sin(\omega t).$$

The period of the harmonic $H(t)$ is defined to be

$$T = \frac{2\pi}{\omega} .$$

A periodic function, $g(t)$, with period T can be arbitrarily closely approximated by the linear approximating polynomial

$$G_n(t) = \sum_{k=0}^{n} [A_k \cdot \cos(\frac{2\pi k}{T} t) + B_k \cdot \sin(\frac{2\pi k}{T} t)]. \qquad \text{(A-4)}$$

The objective is to minimize $\int_0^T [g(t) - G_n(t)]^2 dt$ with respect to the parameter set A_o, A_1, ..., A_n, B_o, B_1, ..., B_n. This is done by setting the partial derivatives

$$\frac{\partial}{\partial A_k} \int_0^T [g(t) - G_n(t)]^2 dt, \quad k = 0, 1, 2, \ldots, n$$

and

$$\frac{\partial}{\partial B_k} \int_0^T [g(t) - G_n(t)]^2 dt, \quad k = 0, 1, 2, \ldots, n$$

equal to zero. Evaluation of the resulting equalities yields the Fourier component representations

$$\hat{A}_k = \frac{2}{T} \int_0^T g(t) \cdot \cos(\frac{2\pi k}{T} t) \cdot dt, \quad k = 0, 1, 2, \ldots, n \qquad \text{(A-5)}$$

and

$$\hat{B}_k = \frac{2}{T} \int_0^T g(t) \cdot \sin(\frac{2\pi k}{T} t) \cdot dt, \quad k = 0, 1, 2, \ldots, n. \quad \text{(A-6)}$$

It has become customary to ignore the "hat" notation in representing $\hat{A}_k$ and $\hat{B}_k$.

It can be shown that, as $n \to \infty$,

$$g(t) \to A_o + \sum_{k=1}^{\infty} [A_k \cdot \cos(\frac{2\pi k}{T} t) + B_k \cdot \sin(\frac{2\pi k}{T} t)]$$

which is usually written as

$$g(t) = A_o + \sum_{k=1}^{\infty} [A_k \cdot \cos(\frac{2\pi k}{T} t) + B_k \cdot \sin(\frac{2\pi k}{T} t)]. \quad \text{(A-7)}$$

The right side of equation (A-7) is called the Fourier series expansion of the periodic function $g(t)$. The coefficients A_o, A_1, . . ., A_n, B_1, . . ., B_n are called the Fourier coefficients of $g(t)$. Note that B_o is equal to zero.

C. Power Spectral Density

Closely related to the concept of the Fourier series representation of a periodic function is the power spectral density representation of a function $f(t)$. However, the power spectral density analysis of $f(t)$ does not require the assumption of periodicity. It constitutes a means whereby hidden periodicities (or near periodicities) within $f(t)$ may be searched for in a systematic way. Thus, the harmonic relation $2\pi k/T$, $k = 0, 1, 2, \ldots$, which is assumed in the Fourier series is not necessary.

To begin with, we define the autocorrelation function of a stationary random process h(t) by

$$R(\tau) = \lim_{T\to\infty} \frac{1}{T} \int_{-T/2}^{T/2} h(t)h(t+\tau)dt, \qquad (A-8)$$

where τ represents the lag of the function. It can be shown that $R(\tau)$ is the integral transform of the power spectram of h(t). That is,

$$R(\tau) = \int_{-\infty}^{\infty} P(f)e^{i2\pi f\tau} \, df \qquad (A-9)$$

where P(f) represents the power spectral density of h(t). Note here that P(f) is a continuous function of frequency, f. The power spectral density is given by the equation

$$P(f) = \lim_{T\to\infty} \frac{1}{T} \left| \int_{-T/2}^{T/2} h(t)e^{-i2\pi ft} \, dt \right|^2. \qquad (A-10)$$

Another important relation involving $R(\tau)$ and P(f) is

$$P(f) = \int_{-\infty}^{\infty} R(\tau)e^{-i2\pi f\tau} \, d\tau. \qquad (A-11)$$

Thus, $R(\tau)$ and P(f) are seen to be integral transform pairs.

In a practical situation, such as measuring river water temperatures, X(t), it is impossible to obtain T → ∞. Only pieces or samples of X(t) are obtainable for finite sample periods. Thus, at most, only estimates of the autocorrelation function and the power spectral density are available.

For continuous records of finite length it is necessary

to use the apparent autocorrelation function given by

$$R_a(\tau) = \frac{1}{T - |\tau|} \int_{-(T-|\tau|)/2}^{(T-|\tau|)/2} h(t - \frac{\tau}{2})h(t + \frac{\tau}{2})dt \qquad (A-12)$$

where

$$|\tau| \leq \tau_m < T.$$

Here τ is the lag, T is the record time, and τ_m is the maximum lag.

The apparent autocorrelation function is next modified by the lag window function, $W_i(\tau)$, having the following properties:

1. $W_i(0) = 1$,

2. $W_i(\tau) = 0$ for $|\tau| > \tau_m$, and

3. $W_i(-\tau) = W_i(\tau)$.

The modified autocorrelation function is thus

$$R_M(\tau) = W_i(\tau) \cdot R_a(\tau). \qquad (A-13)$$

Recalling that the power spectral density and autocorrelation functions are Fourier transform pairs, we obtain the modified power spectral density

$$P_M(f) = \int_{-\infty}^{\infty} W_i(\tau) \cdot R_a(\tau) e^{-i2\pi f\tau} d\tau \qquad (A-14)$$

$$= Q_i(f) * P_a(f)$$

where $Q_i(f)$ is the transform of $W_i(\tau)$ and * is convolution.

The function $P_a(f)$ cannot be obtained since $C_a(\tau)$ is not specified for $|\tau| > \tau_m$. However, the average of $P_M(f)$ is given by

$$\text{ave } [P_M(f)] = Q_i(f) * P(f). \qquad (A-15)$$

At a given frequency f_1, the average of $P_M(f)$ is given by

$$\text{ave } [P_M(f_1)] = \int_{-\infty}^{\infty} Q_i(f_1 - f) \, P(f) df. \qquad (A-16)$$

Thus the true power spectral density $P(f)$ is smoothed and filtered over frequencies near f_1 by the function $Q_i(f_1 - f)$.

In order to show the effect of the lag window, consider first

$$W_o(\tau) = \begin{cases} 1, & |\tau| < T \\ 0, & |\tau| \geq T. \end{cases}$$

This is, in effect, no modification of $R_a(\tau)$ at all since

$$W_o(\tau) \cdot R_a(\tau) = R_a(\tau)$$

Now $Q_o(f)$ is given by

$$Q_o(f) = \int_{-T/2}^{T/2} e^{-i2\pi f \tau} d\tau$$

$$= T \frac{\sin(\pi T f)}{\pi T f},$$

which is of the familiar $\sin(x)/x$ form. Thus the resultant value $Q_o(f_1 - f)$ is a rather poor filter since it has large

side-lobes which allow significant energy to pass at frequencies that are considerably different from f_1.

This gives an indication of the type of function which is needed for $W_i(\tau)$. It is obviously desirable to concentrate the main lobe of $Q_i(f_1 - f)$ near f_1 while keeping the side-lobes as low as possible. Several such functions have been developed including the so-called hanning window which is used in the power spectral analysis presented here. The hanning window is given as

$$W_h(\tau) = \begin{cases} \frac{1}{2}[1 + \cos(\frac{\pi\tau}{\tau_m})], & |\tau| < \tau_m \\ 0, & |\tau| > \tau_m \end{cases}$$

(A-17)

For the hanning window the maximum side-lobe level is about 2 percent of the value at f_1 as compared to about 20 percent for the rectangular window having $\sin(x)/x$ spectral shape.

Since the product, $W_h(\tau) C_a(\tau)$, is the τ domain is equivalent to the convolution, $Q_h(f)*P(f)$, in the frequency domain, it is seen that the weighting factor $W_h(\tau)$ acts as a fixed-bandwidth filter with variable center frequency, f_1. Thus, $D_h(\tau)$ has the effect of smoothing the spectrum by virtue of its reduced side-lobe level.

Since this analysis used a digital computer for numerical calculations, it was necessary to consider the effect on the results caused by sampling of water temperatures at equally spaced intervals. That is, the time-series $X(t_i)$ was analyzed rather than the continuous function $X(t)$. The basic power

spectral density techniques are the same except that now the phenomenon of aliasing must be taken into consideration. The aliasing process is best understood by a consideration of the sampling theorem which is

Theorem

Given that,

(1) h(t) is a real-valued time function, and

(2) h(t) contains no frequency components greater than f_b cycles/(unit of time).

Then h(t) can be completely determined by specifying its ordinates (sampling) at a series of points spaced every $1/2 \ f_b$ units of time.

An alternate way of stating this important theorem is that all the information contained in the frequency band-limited time-domain function, h(t), can be reproduced from the sampled version of h(t), $h_s(t)$, if the sample points are spaced every $1/2 \ f_b$ units of time. The frequency f_b is referred to as the Nyquist frequency.

Now, assuming that the frequency spectrum of h(t), F(t), appears as shown in Figure 29 (a), then the corresponding spectrum of $h_s(t)$, $F_s(f)$, is as shown in Figure 29 (b). The periodic repetition of F(f) is the form $F_s(f)$ is referred to as aliasing. If the sample rate is less than $1/2 \ f_b$, then overlapping (folding) of $F_s(f)$ will occur. This results in misleading information about F(f) at frequencies near f_b.

Note that the amplitude spectrum has been used in the sampling theorem rather than the power spectral density.
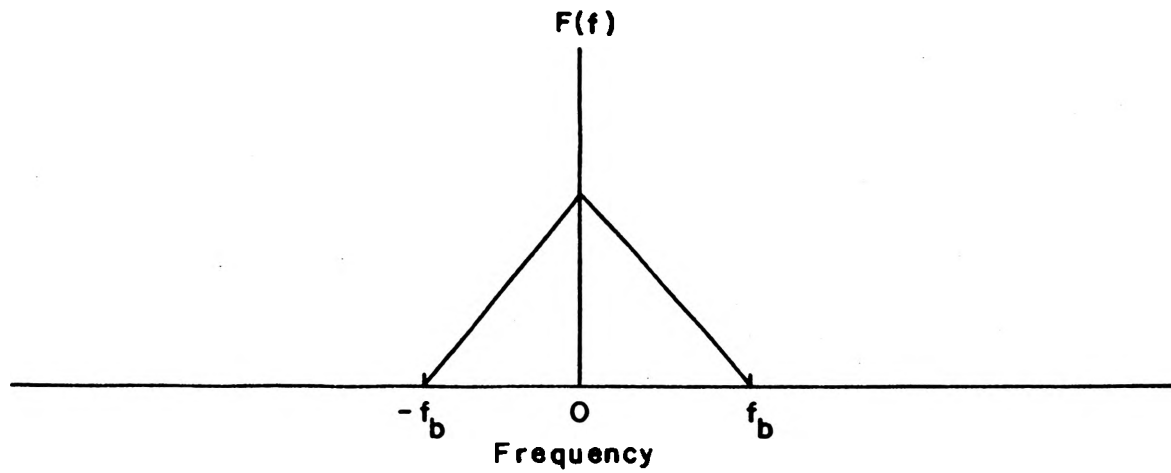
Figure 29 (a). Fourier Transform of Frequency Band-Limited
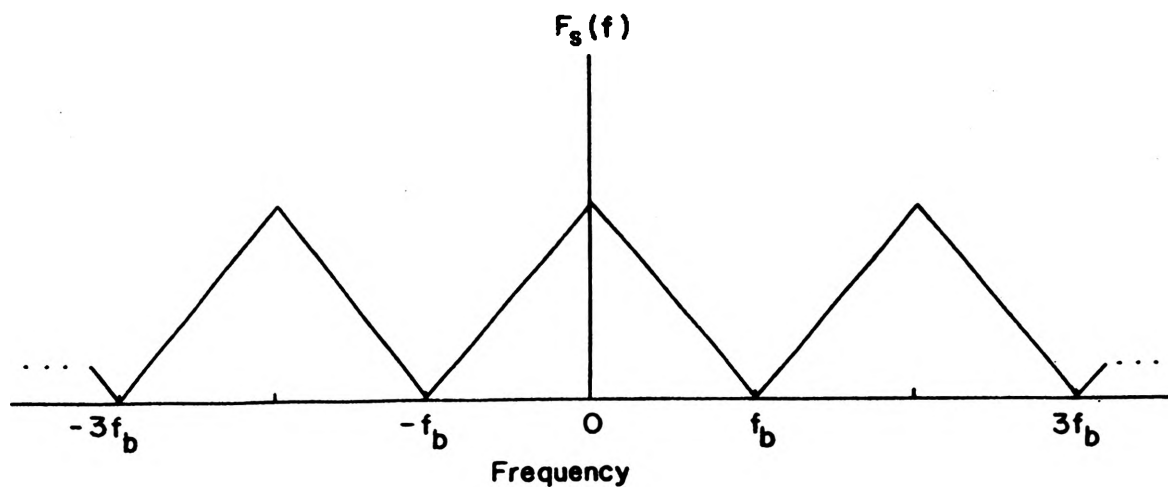Time-Domain Function, f(t).

Figure 29 (b). Fourier Transform of Sampled Version of (a).

However, the aliasing phenomenon is similar since we are now multiplying the sampled version of the autocorrelation function by $W_h(\tau)$ and integrating to obtain the sampled version of the power spectral density. Thus the Nyquist frequency for the power spectral density is given by $f_b = 1/(2 \cdot \Delta\tau)$. But $\Delta\tau = \Delta t$ in practical analyses so that the f_b is the same for both the amplitude spectrum and for the power spectral density calculations. Thus the sample interval must be small enough to insure that no folding of frequencies having significant power levels will occur since the resulting power spectral density calculations will be distorted by the folded power.

With these considerations accounted for we define the sampled version of the apparent autocorrelation function of water temperature samples as

$$\tilde{R}_a(r) = \frac{1}{N-r} \sum_{i=1}^{N-r} X_o(t_i) \cdot X_o(t_{i+r}); \quad r = 0, 1, 2, \ldots, M, \quad \text{(A-18)}$$

where M is the maximum value of the lag number r. In the expression for $\tilde{R}_a$, the function $X_o(t_i)$ represents the zero-average time-series which is obtained by

$$X_o(t_i) = X(t_i) - \overline{X} .$$

The sampled version of the power spectral density estimate is then taken as

$$\text{(A-19)}$$

$$\tilde{P}(f) = 2 \cdot \Delta t \{ \tilde{R}_a(0) + 2 \sum_{r=1}^{M-1} [\tilde{R}_a(r) \cdot \cos(\frac{\pi r f}{f_M})] + \tilde{R}_a(M) \cdot \cos(\frac{\pi M f}{f_M}) \} .$$

This expression for $\tilde{P}(f)$ represents the convolution of the Fourier transform of the sampled autocorrelation function, $\tilde{C}_a(r)$, with the Fourier transform of the sampled version of the weighting function, $W_h(\tau)$.

D. Estimation

The general theory of signal estimation is best considered by observing the model diagram shown in Figure 30. Here the source input is a signal, $a(t)$, which is corrupted by additive noise $\eta(t)$. In most analyses the noise is considered to be a stationary normal random process with zero mean.

If it is assumed that the input is a non-random constant, A, then the total input to the samples is $A + \eta(t)$. Thus, $A + \eta(t)$ has an equivalent probability distribution which is normal with mean equal to A. The sample output is now a set of random samples s_1, s_2, . . ., s_N, from a distribution having probability density function

$$f(s,A) = \frac{1}{\sqrt{2\pi}\sigma} e^{-\frac{1}{2\sigma^2}(s-A)^2} \tag{A-20}$$

The joint p.d.f. of s_1, s_2, . . ., s_N is then the likelihood function

$$L(A, s_1, s_2, \ldots, s_N) = f(s_1,A) \, f(s_2,A) \cdots f(s_N,A)$$

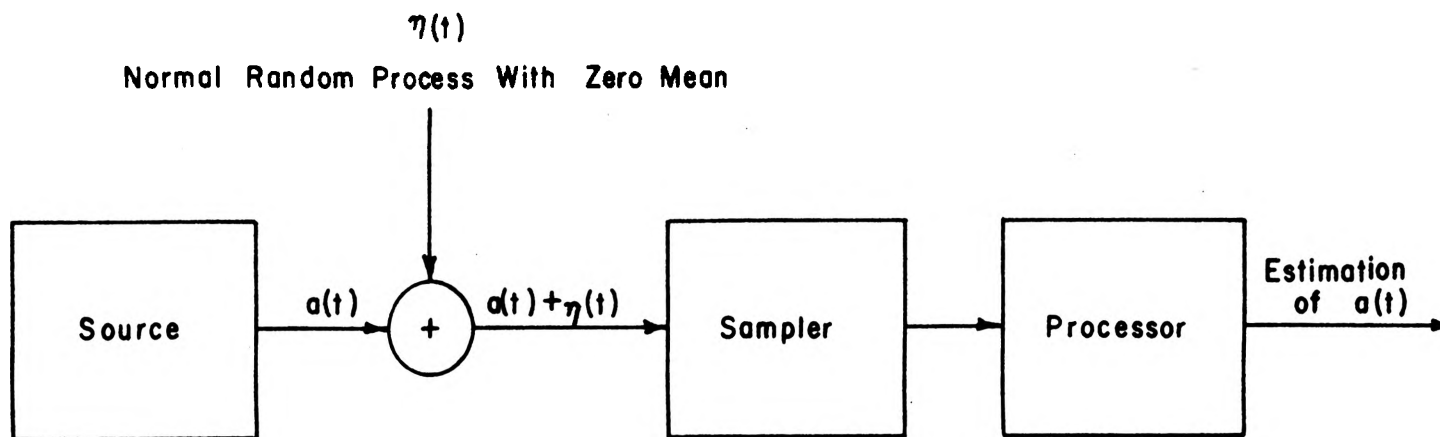$$= (\frac{1}{\sqrt{2\pi}\sigma})^n e^{-\frac{1}{2\sigma^2}\sum_{i=1}^{n}(s_i-A)^2} \tag{A-21}$$

Figure 30. Communication System for Sampling and Estimating Source Output, a(t).

Taking the derivative of $\ln\{L(A, s_1, s_2, \ldots, s_N)\}$ with respect to A gives

$$\frac{d}{dA}\{\ln[L(A, s_1, s_2, \ldots, s_N)]\} = -\frac{1}{2\sigma^2} \sum_{i=1}^{N} (s_i - A)(-2)$$

$$= \frac{N}{\sigma^2}[\frac{1}{N} \sum_{i=1}^{N} (s_i - A)]. \qquad (A-22)$$

Setting this derivative equal to zero gives the maximum likelihood statistic

$$\hat{A} = \frac{1}{N} \sum_{i=1}^{N} s_i \qquad (A-23)$$

for the unknown signal with constant value A. It can be shown that $\hat{A}$ is the unique best statistic for A.

In the estimation process involving thermal inputs to large rivers it is necessary to estimate a constant input in background noise (natural temperature fluctuation) which is far from stationary. However, the background noise consists of at least one large component, the yearly seasonal fluctuation, which is nearly periodic. Hence it will be useful to consider the Fourier series process by which these fluctuations are extracted in view of the previous discussion of estimation.

If the noise is considered to consist of a periodic component having zero average value along with an additive normal random component with zero mean, then

$$\eta(t) = p(t) + r(t) \qquad (A-24)$$

where $p(t)$ is the periodic component and $r(t)$ is the random component. The Fourier components are then

1. $A_{k\eta} = \int_0^T [p(t) + r(t)] \cdot \cos(\frac{2\pi k}{T} t) \cdot dt$ (A-25)

$= A_k + \epsilon_{1k}$

where

$A_k = \int_0^T p(t) \cdot \cos(\frac{2\pi k}{T}) \cdot dt$, and

$\epsilon_{1k} = \int_0^T r(t) \cdot \cos(\frac{2\pi k}{T}) \cdot dt$;

and

2. $B_{k\eta} = \int_0^T [p(t) + r(t)] \cdot \sin(\frac{2\pi k}{T}) \cdot dt$ (A-26)

$= B_k + \epsilon_{2k}$

where

$B_k = \int_0^T p(t) \cdot \sin(\frac{2\pi k}{T}) \cdot dt$, and

$\epsilon_{2k} = \int_0^T r(t) \cdot \sin(\frac{2\pi k}{T}) \cdot dt$.

Thus, an error, which is dependent on the degree of correlation between the harmonics and the noise, exists in the calculated values of the Fourier components. However, the Fourier series still constitutes a minimum mean-square

approximation to the data points which represent the noise function samples, $\eta(t_i)$. This means that, with the extraction of a sufficient number of Fourier components, the noise, insofar as signal estimation is concerned, can be replaced by

$$\eta_e(t_i) = \eta(t_i) - \sum_{k=1}^{n} [A_{k\eta} \cdot \cos(\frac{2\pi k}{T} t) + B_{k\eta} \cdot \sin(\frac{2\pi k}{T} t)]$$

$$\cong r(t_i) \qquad \qquad \text{(A-27)}$$

Thus the signal samples could be preceded by a Fourier component extractor as shown in Figure 31. The assumption must be made that the sample interval is an integral multiple of the period, T, of $p(t)$. With this extraction, the signal processing would then continue with the estimation being made by the maximum likelihood estimation

$$\hat{A} = \frac{1}{N} \sum_{i=1}^{N} [A + \eta_e(t_i)] \ . \qquad \qquad \text{(A-28)}$$

$$\eta(t) = p(t) + r(t)$$

(1) p(t) Periodic

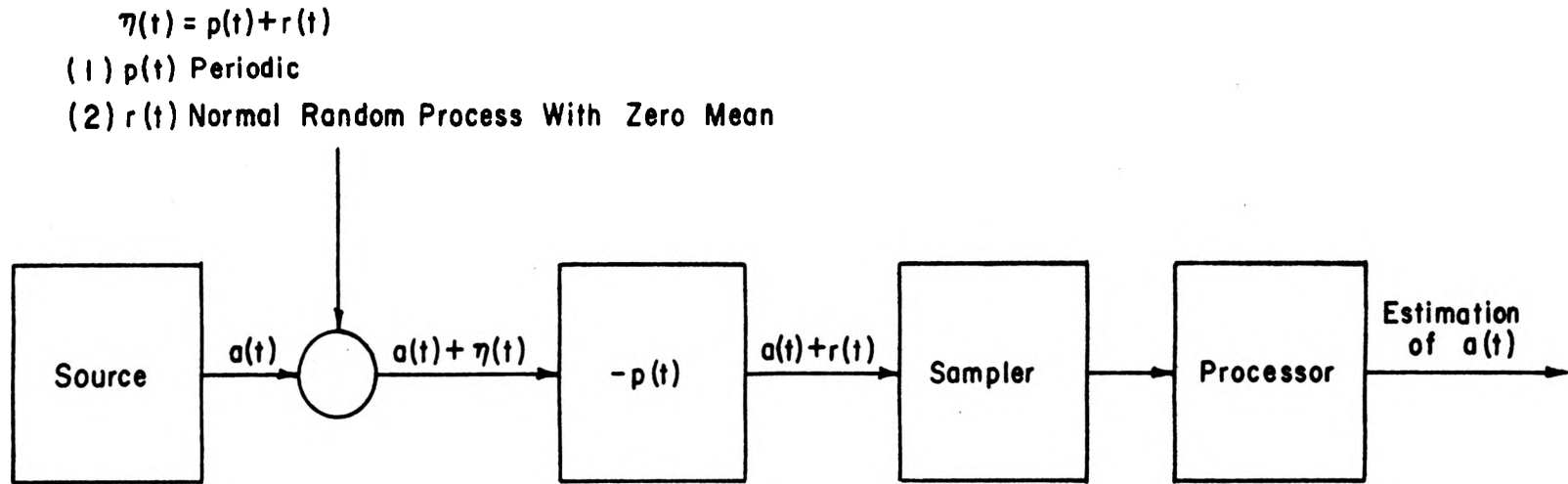(2) r(t) Normal Random Process With Zero Mean

Figure 31. System for Sampling and Estimating a(t) When Corrupted by p(t) + r(t).

APPENDIX B

VERIFICATION OF POWER SPECTRAL DENSITY PROGRAM

Because the power spectral density was used to such a large extent in this dissertation, it is appropriate to justify the correctness of the computer programming technique which was used. The equation

$$\tilde{P}(f) = 2 \cdot \Delta t \{ \hat{R}_a(0) + 2 \sum_{r=1}^{M-1} [\tilde{R}_a(r) \cdot \cos(\frac{\pi r f}{f_M})] + \tilde{R}_a(M) \cdot \cos(\frac{\pi M f}{f_M}) \}$$

was programmed using FORTRAN IV. As a test, several known input time functions were used to generate data having cyclic components. All results verified the correctness of the programming as well as the use of the equation.

Typical of the results which were obtained is the power spectral density plot shown in Figure 32. Here the input signal was

$$s_i(t) = 10 \cos(2\pi \cdot 20t) + 5 \sin(2\pi \cdot 40t) .$$

Data was generated by sampling this signal 365 times at equal intervals for a total time period T equal to one (year). It should be noted in particular that the side-lobe level is insignificant in this case.